UNDERSTANDING THE EFFECTS OF LONG-DURATION SPACEFLIGHT ON FRACTURE RISK IN THE HUMAN FEMUR USING FINITE ELEMENT MODELING

A Thesis

presented to

the Faculty of California Polytechnic State University,

San Luis Obispo

In Partial Fulfillment

of the Requirements for the Degree

Master of Science in Mechanical Engineering

by

Keyanna Henderson

December 2020

COMMITTEE MEMBERSHIP

TITLE:	Understanding the Effects of Long-Duration Spaceflight on Fracture Risk in the Human Femur Using Finite Element Modeling
AUTHOR:	Keyanna Henderson
DATE SUBMITTED:	December 2020
COMMITTEE CHAIR:	Scott Hazelwood, Ph.D. Professor of Biomedical Engineering
COMMITTEE MEMBER:	Joseph Mello, Ph.D. Professor of Mechanical Engineering
COMMITTEE MEMBER:	Peter Schuster, Ph.D. Professor of Mechanical Engineering

ABSTRACT

Understanding the Effects of Long-Duration Spaceflight on

Fracture Risk in the Human Femur Using Finite Element Modeling

Keyanna Henderson

Long-duration spaceflight has been shown to have significant, lasting effects on the bone strength of astronauts and to contribute to age-related complications later in life. The microgravity environment of space causes a decrease in daily mechanical loading, which signals a state of disuse to bone cells. This affects the bone remodeling process, which is responsible for maintaining bone mass, causing an increase in damage and a decrease in density. This leads to bone fragility and decreases overall strength, posing a risk for fracture. However, there is little information pertaining to the timeline of bone loss and subsequent fracture risk.

This study used finite element analysis to model the human femur, the bone most adversely affected by spaceflight, and to simulate the environments of Earth preflight, a six-month mission on the International Space Station, and one year on Earth postflight. Changes in the properties of cortical and trabecular bone in the femoral neck were measured from the simulations, and used to provide evidence for high fracture risk and to predict when it is most prominent.

It was found that a risk for fracture is extremely evident in the femoral neck in both cortical and trabecular bone. Cortical bone in the inferior neck exhibited high magnitudes of damage, while the superior neck suffered the greatest increases in damage that proceeded to increase upon return to Earth. The density of trabecular bone decreased the most significantly and was not fully recovered in the following year. While it is still unclear exactly when these changes cause the greatest risk for fracture, it is possible that they will add to and advance the onset of medical complications such as osteoporosis. Additionally, the results of this study support the claim that the current countermeasure of inflight exercise is insufficient in sustaining bone mass and preserving skeletal health. The effects of long-duration spaceflight on bone health should continue to be investigated especially if future missions are to last as long as one to three years.

Keywords: Bone loss, bone remodeling, spaceflight, fracture risk, finite element analysis

ACKNOWLEDGMENTS

Thank you to the best advisor, Dr. Scott Hazelwood, for an entire year of thoughtful guidance and enthusiastic support. Challenges and all, I had a lot of fun and learned so much through this project. Additional thanks to Dr. Joseph Mello and Dr. Peter Schuster for readily joining the team and providing their helpful insight.

Finally, thank you to my family for their love and support, and for always cheering me on.

TABLE OF CONTENTS

Page

LIST OF TABLES

Table Page

LIST OF FIGURES

Figure Page

1. INTRODUCTION

1.1 Motive

It has been shown that long-duration spaceflight has significant effects on bone loss and damage accumulation and can contribute to fracture risk upon return to Earth or later in life [1]. This is thought to occur in astronauts embarking on missions six months or longer, in both orbit and on the International Space Station (ISS). The microgravity environment of space presents either an absence of loads or a significant decrease in loads, representing a state of disuse. This adversely affects the process of bone remodeling, which is responsible for maintaining bone mass at equilibrium, leading to bone loss. This loss is most accurately captured by changes in volumetric bone mineral density (vBMD). The time course of bone loss and fracture risk is still uncertain, however. It is possible that bone loss could lead to fracture risk during flight, immediately upon return, or later in life due to age-related complications.

Bone damage as a result of spaceflight also contributes to these effects and is likely to further increase fracture risk [2] [3]. It has been observed that damage accumulates when bone remodeling is suppressed in microgravity environments, reducing bone toughness and decreasing resistance to fracture. However, due to a lack of data, the relationship between damage and fracture risk is not clear [4].

Studies have shown that crewmembers on the ISS experience a considerable loss of bone in the cortical and trabecular regions of the hip and a smaller loss in the spine [5]. Many have determined that the proximal femur endures the most severe bone loss in space [6]. Because the femur is also known to experience natural, medical complications later in life, such as osteoporosis and fractures of the femoral neck, this bone loss can be detrimental.

While countermeasures to this bone loss have been made in the form of several pharmaceutical methods, the primary tool remains to be in-flight exercise. It has been the most frequently attempted and has proven to be effective for several physiological systems [7]. However, it has not been successful in entirely preventing bone loss.

1.2 Bone Remodeling

Bone remodeling is the continuous, biological process which removes old bone and replaces it with new tissue [8]. In addition to maintaining bone mass, remodeling removes microdamage and modifies bone structure in response to stress, strain, and mechanical loads. The process is carried out by basic multicellular units (BMUs), which are teams of cells comprised of osteoclasts and osteoblasts. Osteoclasts are responsible for resorbing packets of bone and osteoblasts are responsible for refilling the cavities left by osteoclasts [9]. The teams of cells work together in BMUs to constantly form new tissue and resorb old bone, maintaining bone mineral homeostasis. The remodeling process is generally activated when cells sense changes in mechanical strain placed by loads of daily activity and translate them into biological signals [10]. It is also initiated when new BMUs are activated in response to damage, which can result from a wide range of loads on bone [11].

The remodeling cycle takes three to four months to complete, and in the meantime, cavities formed by the process can temporarily add to bone's porosity. This "remodeling space" can be small, but substantial in weakening the structure of bone [9]. This is referred to as the "time lag" of bone remodeling and in critical environments such as space, it can be detrimental to bone health. If cavities are not being filled as quickly as they are being made, bone mass and strength can severely decrease and cause fracture risk.

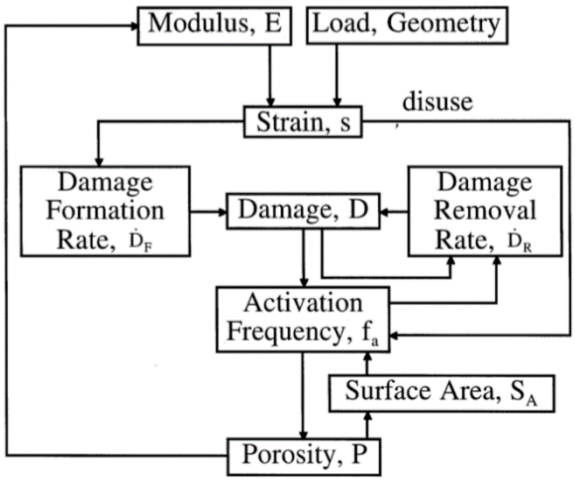

Figure 1. Schematic Representation of Bone Remodeling Process and Feedback Loops [9]

An important parameter of bone remodeling is BMU activation frequency, which measures the number of new BMUs per unit area of bone per unit of time. Figure 1 shows the feedback loops of bone remodeling, in which BMU activation frequency is caused by load-induced disuse and microdamage in the bone tissue. By creating a model that simulates the microgravity environment of space and interpreting changes in material properties, it can be determined how the process of remodeling is affected and the consequences it has on bone.

1.3 Spaceflight

The environment of microgravity in space is often referred to as having “zero gravity” due to the feeling of weightlessness it creates [12]. Gravity, however, does exist in space and all people and objects are indeed in a state of free fall. The gravitational field is still strong at the altitude in which shuttles orbit and the ISS resides – it is just less than that on Earth. At the altitude of the ISS, between 200 and 250 miles from the surface of Earth, gravity is about 90% of that on Earth [13] [14]. It appears that people and objects are floating and not falling because they are kept in orbit by gravity and are actually falling “around” Earth. This is because gravity pulls on objects in space just as it does on Earth, but at an extremely fast speed – approximately 17,500 miles per hour. Spacecrafts in orbit, such as the ISS, are designed to move at a speed such that the curve of their fall matches the curve of the Earth’s surface. As a result, they continuously fall around the planet, and not towards it as objects do on Earth [13].

The decrease in gravity makes exercising in space especially critical in maintaining bone health of crewmembers. It typically results in a larger amount of time spent exercising to compensate for the lack of skeletal loading normally felt on Earth. Additionally, the feeling of weightlessness makes standard exercising impossible and requires the use of equipment specifically designed for space. An observational study by Trappe et al. documented the exercise regime of crewmembers aboard the ISS for six months [15]. It was prescribed to the crewmembers that they exercise 2.5 hours (including setup, stowage, and personal hygiene) per day, six to seven days per week. The equipment options included a treadmill with a vibration isolation system, bicycle ergometers, an interim resistive exercise device (iRED), and bungee cords. A study by Cavanagh

[16] documented a similar routine and the same use of equipment among members of another expedition aboard the ISS. In both cases, the regimen was not fixed and crewmembers were permitted to exercise as they chose with the guidance of trainers and staff.

Although some pharmaceutical preventative measures have been implemented in spaceflight, they have not been routinely used or heavily studied. Treatments such as bisphosphonates, testosterone, vitamin K, vitamin D, and calcium have been investigated in small case studies of astronauts and animals [17]. While these have been shown to have positive effects on stabilizing bone metabolism, it is still uncertain whether they can completely prevent bone loss from occurring. Additionally, there is insufficient data to prove the efficacy of pharmaceutical treatments in preventing the development of osteoporosis. Exercise remains to be the primary countermeasure for bone loss in space. Therefore, as the length of missions extends in future expeditions, it is necessary to determine if the current forms and quantities of exercise are sufficient.

As more missions have been completed, there has been an increase in available data, allowing people to conduct improved studies on the effects of spaceflight on bone health. Using a variety of methods, researches are using pre- and postflight data to better understand changes in the properties of bone that occur during flight and how they are influenced by factors such as exercise and pharmaceutical measures. They are also interpreting results to predict how bone is negatively affected by spaceflight later in life.

A study by Keyak et al. [18] used quantitative computed tomography (QCT) scan-based, finite element modeling and dual-energy X-ray absorptiometry (DXA) to quantify changes in femoral areal bone mineral density (aBMD) and bone strength in 13 astronauts making 4.3- to 6.5-month missions to the ISS. While aboard the ISS, astronauts followed their own exercise program which consisted of two-hour sessions, four days per week. QCT scans were taken pre- and postflight, segmented, and generated into finite element models. The models were then analyzed under loading conditions for a single-limb stance and for a fall to the greater trochanter. It was found that density decreased for all astronauts, and strength decreased for all under single-limb stance loading, and for all but two under fall loading. The decrease in strength for some individuals was

comparable to average lifetime losses in Caucasian females. While this experiment was strong and the results valid, there were some limitations in the model. Because bone properties were calculated based on scans, they did not account for temporal or local changes. Additionally, the experiment only measured changes immediately postflight, and did not consider changes that occurred after having returned to Earth for an extended period of time.

A similar experiment by Lang et al. [5] also used QCT and DXA to measure cortical and trabecular bone loss in the spine and hip of 14 astronauts making 4- to 6-month missions on the ISS. Scans were taken of the hip, spine, and heel pre- and postflight and processed to extract measurements for vBMD, bone mineral content (BMC), and bone volume. In the femur, regions of interest included cortical, trabecular, and integral (cortical and trabecular combined) bone in the neck. Percent changes were calculated between pre- and postflight values, as well as the percent changes per month. Both cortical and trabecular bone density decreased significantly, with a larger change occurring in trabecular bone. This study was strong in that it provided insight for changes in specific skeletal sites and for different bone types, but it still had some weaknesses. It used partial volume averaging for cortical bone measurements, which refers to the small size of the object being measured relative to the spatial resolution of the measurement device. Like the experiment by Keyak et al. [18], this study only accounted for changes between pre- and immediately postflight.

Another study that should be mentioned is that of Gardina [19], who used a computer model and bone remodeling algorithm to simulate the effects of spaceflight on human bone with and without the use of bisphosphonate therapy. Bisphosphonates are a drug used to combat bone loss through the alteration of the bone remodeling process. Gardina produced simulations for missions lasting between 10 days and one year, with and without bisphosphonates, and collected data for density and bone damage accumulation. The model exhibited significant changes in density and damage as a result of spaceflight, as well as continuing changes after returning to Earth as remodeling readjusted. Bone density decreased in spaceflight in all scenarios and damage increased in spaceflight, and long after returning to Earth. The results of the study found treatment to increase bone mass and reduce fracture risk. It predicted that without treatment, complete

recovery would not occur. This study was strong in that it modeled bone behavior for varying periods of time in space as well as extended periods of time after flight. However, because it did not use a physical model of a specified bone structure, it did not provide as accurate of a remodeling response as a finite element model would have. Additionally, the model was simplified in that it did not consider biological factors such as blood flow, drug metabolism, and hormonal levels, which could influence the efficacy of treatment with bisphosphonates.

1.4 Objective

The objective of this study is to use finite element modeling to understand the effects of spaceflight on several properties of human bone and its correlation to fracture risk. By using a finite element model, the results will be more accurate and provide visual inference for changes in bone properties. This will be achieved by simulating the environments of Earth preflight, spaceflight, and Earth postflight. Spaceflight conditions will be created to match that of a six-month mission to the ISS, the average length of missions to date [20]. The femur bone will be modeled as it experiences the greatest effects in space, and changes in properties will be calculated in the neck region for both cortical and trabecular bone as it is most prone to fracture naturally [5]. This will allow results to be interpreted separately for the very different types of bone. Additionally, the study will provide inference as to whether the current in-flight exercise regimen used by crewmembers is sufficient in maintaining bone health.

2. METHODS

2.1 Model Development

To model the effects of spaceflight on the adult femur, a three-dimensional, whole bone model was used that was originally created by Christopher Deuel [21] combined with a bone remodeling algorithm developed by Hazelwood et al. [9] for a fatigue damage removal study. The algorithm was created to accurately simulate bone remodeling and to provide a better understanding of bone's response to disuse and overload. Loads are placed on the bone and the resulting strain determines stimuli which then estimate disuse and damage. These activate bone remodeling through the simulation of basic multicellular units (BMUs or teams of osteoclasts and osteoblasts), which are responsible for carrying out the processes of adding or removing bone. The mechanistic algorithm exhibits changes at each step in time of several material properties. The results of the study by Hazelwood et al. indicated that the algorithm may be useful in predicting and understanding transient responses for bone in a low gravity state, such as space.

The algorithm developed by Hazelwood et al. [9] was later used in the dissertation of Deuel [21]. Deuel incorporated the algorithm into a three-dimensional, finite element model of the femur that would simulate the femur's response in bone remodeling to different types of hip implants: a hip resurfacing implant versus that of a conventional femoral stem used in total hip arthroplasty. By integrating the relationships defined by Hazelwood's algorithm into a finite element model, the changes in material properties may be accurately measured at any location of the femur, despite the complicated geometry of the bone and/or implant.

2.2 Finite Element Model

To create the geometry and mesh of the femur model, Deuel [21] used a computed tomography (CT) scan of the femur from an adult male cadaver whose soft tissues were removed. From the CT scan a two-dimensional, triangular surface mesh was created using Mimics, and from that mesh a three-dimensional, quadratic tetrahedral mesh was created using Patran. Quadratic tetrahedral elements were selected for their ability to produce an accurate mesh with minimal

processing time. Additionally, they are likely to be the best option when a solid model of the object of interest is available [22]. Deuel then performed a convergence study on five different meshes of varying element size to determine the best mesh density. The final model was chosen by placing simplified loads of the joint and abductor muscle forces on the model, comparing differences of strain and displacement between the models, and identifying the convergence of strain and displacement outputs. The final mesh used by Deuel and in this study consisted of 29,175 elements and 41,723 nodes.

After creating the model, Deuel [21] implemented the bone remodeling algorithm created by Hazelwood et al. [9] by defining a user material subroutine. Because the algorithm includes the activity of BMUs, the subroutine allows for the model to respond to different loading schemes as bone would in a natural environment.

2.3 Bone Remodeling Algorithm

In the bone remodeling algorithm created by Hazelwood et al. [9] and integrated by Deuel [21] into the finite element model through a UMAT user subroutine, remodeling is activated by loads that are too low and signal disuse, and by repetitive loads that result in damage. Because it uses a whole bone model, the algorithm allows for remodeling to occur simultaneously as a result of both of these cases in different, local areas of the bone. The two-stage process of remodeling is accomplished through two types of cells: osteoclasts responsible for the resorption of bone and osteoblasts responsible for the refilling of bone cavities. It typically requires three to four months to complete the remodeling process by BMUs and in the intervening time, cavities can contribute to temporary porosity and decrease bone strength.

The algorithm calculates changes at each step in time for nine state variables. They are the mechanical stimulus, damage, number of resorbing BMUs, number of refilling BMUs, BMU activation frequency, normalized specific surface area, porosity, elastic modulus, and strain. The mechanical stimulus (Φ) is the forcing function responsible for signaling disuse and driving the remodeling process.

Measured in cycles per day, it is a function of principal strain and loading cycles of n different daily activities. It is calculated using Equation 1,

$$\Phi = \sum_{i=1}^{n} s_i^q R_{Li} \qquad \text{Eqn. 1}$$

where s is the product of the strain range of an activity, raised to the power of q, multiplied by the loading rate (R_L) of that activity, measured in cycles per day. The value of q is 4, the selection of which was based on a study by Whalen and Carter [23].

The initial mechanical stimulus was estimated from the strain needed to maintain (keep resorption and formation in equilibrium) cortical bone mass in a person experiencing 3,000 cycles per day of lower extremity loading [9]. Disuse is then defined as when the stimulus is less than that of the initial value. The mechanical stimulus, when multiplied by a damage rate coefficient, is also used to calculate the damage formation rate, where damage is equivalent to the total crack length per section area of bone (mm/mm^2).

BMU activation frequency, a function of the number of BMUs activated by disuse and damage per area per time ($BMUs/mm^2$/time), is equal to the sum of BMUs activated by disuse and damage, multiplied by the normalized specific area (internal surface area per unit volume). The rate of change of porosity is then assumed to be a function of the mean rates of these refilling and resorbing BMUs, as well as the density of the BMUs (number of BMUs per area) currently active. Changes in porosity are calculated at each time step based on these remodeling characteristics. The elastic modulus, measured in MPa, is assumed to have a nonlinear relationship with porosity (p), and is calculated using Equation 2 for cortical bone, and Equation 3 for trabecular bone.

$$E = 23440(1-p)^{5.74}\ (\text{MPa}) \qquad \text{Eqn. 2}$$

$$E = 14927(1-p)^{1.33}\ (\text{MPa}) \qquad \text{Eqn. 3}$$

Because the algorithm simulates the behavior of BMUs, and variables activated in response are measured at each step in time, the model is able to adapt over time in local areas as a result of disuse and damage.

2.4 Forces

In addition to the implementation of Hazelwood's algorithm, Deuel [21] applied loads to the model that mimicked joint and muscle forces experienced during walking and stair climbing on a daily basis. This consisted of three loading cases representing the heel strike phase of walking, the toe-off phase of walking, and the maximum force of stair climbing. These three load cases were then repeated daily for the desired time period. Based on the typical activity level of a patient with a total hip arthroplasty, the walking forces in Deuel's model were applied for 2,500 cycles per day per leg and the stair climbing force for 20 cycles per day. The magnitudes and directions of these joint forces in the x-z plane were based on a one-legged stance loading study by McLeish and Charnley [24]. The forces were calculated using a body weight of 836 N, also based on that of the typical patient with a total hip arthroplasty, as determined by Bergmann et al. [25] in a study on hip contact forces from routine activity. The direction of the forces in the x-y plane were also taken from Bergmann et al. The magnitudes of these joint forces were 2,091 N for walking and 2,258 N for stair climbing. In an effort to simplify the model, Deuel also applied the loads to the muscle groups having the greatest influence on strain and remodeling. As shown and labeled in Figure 2, this consisted of the gluteus medius, gluteus minimus, adductor longus, adductor brevis, psoas, vastus lateralis, and vastus medialis [21]. A table containing the magnitudes of the loads can be found in Appendix A. Lastly, the model was constrained at the distal (bottom) end of the femur.

The forces were then applied to the model and the simulation was run until it reached a steady state in which the remodeling parameters of porosity, damage, and activation frequency experienced a change of less than five percent over 30 iterations. This occurred after a loading period of 700 iterations, after which the model was determined to resemble that of a skeletally mature femur.

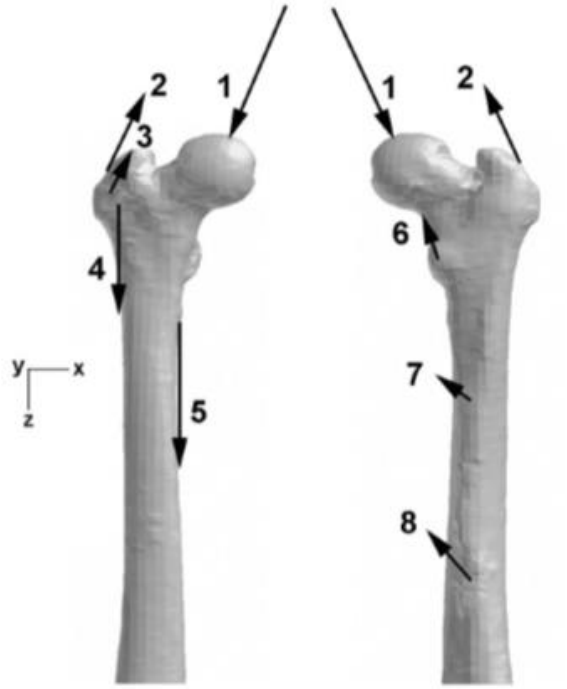

Figure 2. Joint and Muscle Forces Application Locations [1. Hip joint, 2. Gluteus medius, 3. Gluteus minimus, 4. Vastus lateralis, 5. Vastus medialis, 6. Psoas, 7. Adductor brevis, 8. Adductor longus] [21]

2.5 Thesis Model

The femur model of Deuel [21] was used in this thesis study to conduct a quasi-static analysis of an adult femur before, during, and after traveling to the ISS for six months. This was accomplished by modifying the model and algorithm to produce simulations on Earth, in space, and back on Earth after flight. The bone remodeling algorithm was incorporated into the finite element model through a UMAT user subroutine. Data were then collected from each simulation for changes in state variables that would represent the effects of spaceflight on the femur for the two primary types of bone: cortical and trabecular. The first state variable of interest was porosity (p), from which bone area fraction, equal to 1 – p, was calculated. Bone area fraction (BAF), representative of bone volume per total volume (assumed to be equivalent to bone area per total area), was used to calculate density (ρ) by multiplying BAF by the density of bone tissue in the proximal femur: 2.11 g/cm^3 (Equation 4) [26].

$$\rho = 2.11(\mathrm{BAF})\ \mathrm{g/cm^3} \qquad \text{Eqn. 4}$$

The second state variable of interest was bone damage. To better compare the changes in damage between cortical and trabecular bone, damage was divided by bone area fraction to represent damage per bone tissue area, as opposed to total area. The third and final state variable of interest was activation frequency of the bone cells (BMUs). All analyses in this study and that of Deuel's were performed using Abaqus (Simulia, Providence, Rhode Island).

2.6 Earth Baseline Simulation

The first step of this analysis was to bring the model of the femur to a steady state form, resembling that of a skeletally mature adult – specifically that of the typical astronaut. This was accomplished with an Earth baseline simulation. The Earth baseline simulation was produced by applying the walking and stair climbing loads, determined by Deuel [21] and shown in Appendix A, to the finite element model. However, to better simulate the femur of an astronaut, the forces for an individual weighing 836 N (equivalent to 188 lbs. – a value permitted for spaceflight according to NASA's physical requirements [27]), were instead applied 5,000 cycles per day (per leg) for walking and 40 cycles per day (per leg) for stair climbing. This corresponds to a total of 10,000 steps per day – a fair approximation for the active, athletic lifestyle of an astronaut [28]. An equilibrium state was achieved for this simulation after 700 iterations and data were collected for damage per bone tissue area, BMU activation frequency, and density.

2.7 Earth Baseline Simulation Validation

For the purpose of validating the Earth baseline results, the dissertation of Deuel [21] was used. As a part of his study, Deuel conducted an experiment in which strain magnitudes were measured on the surfaces of cadaveric femurs under loading conditions representative of the single-leg stance phase of walking [29]. The experiment, performed using a material testing machine, used multiple strain gauges, load cells, and a custom-made fixture which applied a joint contact force and abductor muscle force. The distal (bottom) end of the femur was rigidly constrained using potting cement. Using a data acquisition system, strain was measured and

averaged at four regions on the femur: proximomedial, proximolateral, distomedial, and distolateral. The test was repeated three times to provide consistency in results and ensure repeatability.

The Earth baseline simulation for this thesis was validated by comparing its results to those of Deuel's [21] experimental study. The Earth baseline placed everyday walking and stair climbing loads on the femur, which was constrained at the distal end, until material properties reached equilibrium. Loads equivalent to the Deuel study were then applied to the baseline model and strains were measured and averaged in the same four regions, and compared to those of Deuel's [29] experiment.

The Earth baseline simulation was further validated by comparing its results for density to experimental studies by Yeni et al. [30] and Morgan et al. [26]. Yeni et al. conducted an investigative experiment of cortical bone in the femoral neck to understand the relationship between fracture toughness (resistance to crack growth) and age, microstructure, and composition. Fracture toughness was studied for its reliable indication of bone fragility and the femoral neck was selected for its susceptibility to fracture. Using a computer numerical control (CNC) milling machine, bulk sections were removed from the posterior and inferior sections of the femora, planed and notched, and then pre-cracked. They were then tested in a servo-hydraulic load frame and fracture toughness was calculated from the results. After testing, samples were cut from the bulk sections, measured, and hydrated to collect their wet weights and densities. They were further treated accordingly to collect dry data as well as measurements of several parameters. The averaged data from Yeni et al.'s study for wet density of the inferior neck section was used to validate the results for bone density in the inferior neck region (Figure 3) from the Earth baseline simulation. Because the femur in the finite element model used in this thesis is that of a male, the value used from Yeni et al. is the average for the male specimens.

Figure 3. Region of Cortical Bone in Inferior Femoral Neck of Model

Morgan et al. [26] conducted a study in an effort to observe the relationship between anatomic sites and density of trabecular bone in the vertebra, proximal tibia, femoral greater trochanter, and femoral neck. The experimental study randomly assigned cadaveric tissue to tensile or compressive testing and used a servo-hydraulic load frame to apply strain cycles. Strain was then measured using an extensometer and modulus was measured from the stress-strain curve. After testing, the tissue was cleaned and wet density was calculated. The average wet density found by Morgan et al. was used to validate the result for the bone density of trabecular bone (Figure 4) in the femoral neck from the Earth baseline simulation.

Figure 4. Region of Trabecular Bone in Femoral Neck of Model

2.8 Space Simulation

After the model was brought to an equilibrium state with the Earth baseline simulation, the space simulation was produced. The joint force and muscle loads used for the Earth baseline were scaled to 90% of their original values to simulate the microgravity environment of the ISS [14]. This also accounts for the resistance felt by astronauts while exercising 2.5 hours per day, six to seven days per week. The scaling of joint and muscle forces to 90% was used in several other studies and simulations, including that of Gardina [19]. The scaled loads can be found in Appendix B. A daily step count of 10,000 (5,000 cycles per leg per day) was used again to account for the extensive amount of exercise performed by crewmembers in space [28] [15]. The simulation was run for six months to match the average trip length of astronauts traveling to the ISS [20]. Data was collected upon completion of the simulation (i.e. immediately upon return from space) for damage, BMU activation frequency, and density.

2.9 Space Simulation Validation

The results of the space simulation were validated by comparing them to the results of Lang et al. [5] who performed a study that used volumetric quantitative computed tomography (vQCT) to measure cortical and trabecular bone loss of the femur in crewmembers making four to six-month flights on the International Space Station. vQCT was used to create cross-sectional images of the proximal femoral neck which were then calibrated to measure cortical and trabecular vBMD. These measurements were taken from a 2-mm-thick section constructed from the scans containing the smallest cross-sectional area of the femoral neck. By performing pre- and postflight measurements with these images they were able to quantify the amount of bone loss that occurred in space by percent change per month, as well as the initial and final values.

The space finite element model of this thesis was validated by performing a simulation mimicking the study of Lang et al [5]. This consisted of beginning with the results of the Earth baseline simulation and then performing a simulation of six months in space. The locations from which to collect data were then determined by selecting a region of elements that matched the regions of cortical and trabecular bone measured in the Lang et al. study. For cortical bone, this

included the inferior and superior regions of the femoral neck (Figure 5). The region of trabecular bone matched that of the Earth baseline simulation validation in Figure 4.

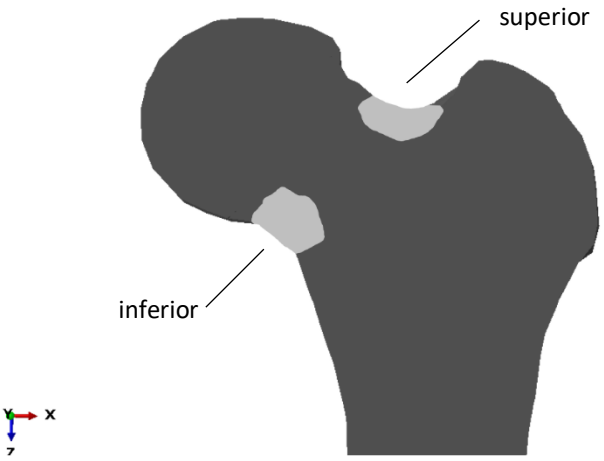

Figure 5. Region of Cortical Bone in Inferior and Superior Femoral Neck of Model

Data were then obtained for the density values of these regions corresponding to the steady state values produced by the Earth baseline simulation and at the end of the six months in space. Changes in density were then calculated for each region to compare values for the percent change per month to those of Lang et al. [5].

2.10 Postflight Simulation

Upon completion of the six-month space simulation, a final, postflight simulation was produced to again simulate life on Earth in order to study the immediate and delayed effects of spaceflight. The joint force and muscle loads from the Earth baseline model were scaled back to their original values and the daily step count was maintained at 10,000 (5,000 cycles per leg per day). This simulation was run for twelve months to provide the most accurate results and extensive understanding of the femur's behavior upon returning to Earth from space. This duration also ensured that the bone remodeling cycle, which typically takes three to four months, would be completed several times. Data were then collected once every thirty days for damage, BMU activation frequency, and density.

3. RESULTS

3.1 Earth Baseline Simulation Validation

To validate the Earth baseline simulation, strain was measured in four regions of the femur, proximomedial (PM), proximolateral (PL), distomedial (DM), and distolateral (DL), and compared to the results of Deuel's [29] experiment. Figure 6 shows a contour plot of strain in the model after the Earth baseline simulation, representing strain in the femur at its equilibrium state. The regions from which strain was measured and averaged are identified.

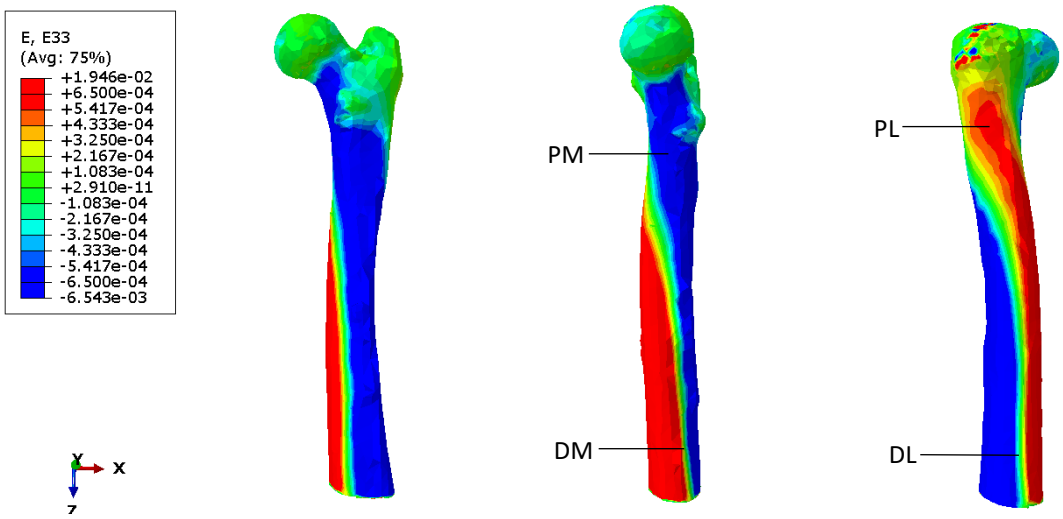

Figure 6. Contour Plot of Strain in Model After Earth Baseline Simulation

The average values for strain in each region are shown in Table 1, with the results from Deuel's [29] experiment. The values from the earth baseline for the proximomedial and distomedial regions are within one standard deviation of Deuel's values, and the values for the proximolateral and distolateral regions are within two standard deviations. Larger differences between the values are likely to be attributed to the high number of loading cycles in the model, which was likely to be much higher than the number of daily steps taken by the individuals whose cadaveric femurs were used in the experimental study. The accuracy of the results serves to validate the earth baseline simulation.

Table 1. Comparison of Earth Baseline to Deuel [29] Experiment for Regional Mean Strain (standard deviation in parenthesis, negative strain is compressive, positive strain is tensile)

		Deuel Experiment	Earth Baseline
Microstrain (με)	Proximomedial	-621 (96)	-561
	Proximolateral	637 (59)	520
	Distomedial	40 (35)	36
	Distolateral	-126 (57)	-62

The Earth baseline simulation was further validated using its results for density. For cortical bone, the study by Yeni et al. [30] was compared against bone density in the inferior region of the femoral neck. The study by Morgan et al. [26] was used to validate the results for bone density in the trabecular region of the femoral neck. A contour plot of density after the simulation is shown in Figure 7, in which the two types of bone used to validate the model, cortical bone in the inferior neck region and trabecular bone, are identified. The contour plot shown and all other two-dimensional contour plots included in this report are cross-sectional images, created to depict the smallest cross-sectional area of the femoral neck. The density distribution produced by the model very closely resembles that of a skeletally mature femur. Dense cortical bone is on the edges of the shaft of the model representing the cortical bone of the diaphysis (shaft) of the femur. The medullary canal, the central cavity where marrow is stored, is visible in the center of the bone shaft, encased by this dense outer shell of cortical bone. Trabecular bone is much more porous and makes up much of the inside of the proximal femur, as is expected.

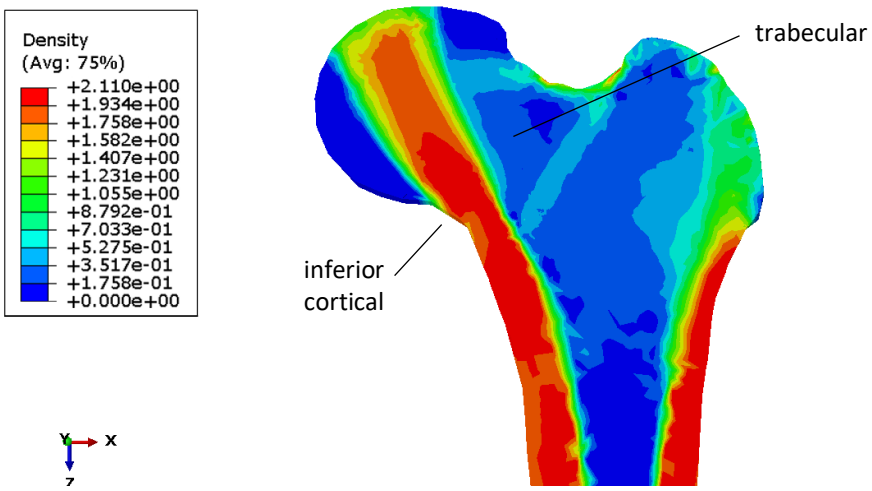

Figure 7. Contour Plot of Density (g/cm3) after Earth Baseline Simulation

The result for cortical bone density in the inferior neck region of the model (1.995 g/cm^3) is shown in Table 2, with the value from the study by Yeni et al [30] (1.91 g/cm^3). The values are similar, with the density from the Earth baseline being nearly within one standard deviation of Yeni's, validating the Earth baseline simulation.

Table 2. Comparison of Earth Baseline to Yeni et al. [30] for Cortical Density (standard deviation in parenthesis) in Inferior Neck Region

	Yeni et al. Study	Earth Baseline
Density (g/cm^3)	1.91 (0.08)	1.995

The model result for trabecular bone density (0.501 g/cm^3) is shown in Table 3, with the value from the study by Morgan et al [26] (mean density of 0.56 g/cm^3). The value from the Earth baseline is within the range of Morgan's density measurements, further validating the density results of the simulation.

Table 3. Comparison of Earth Baseline to Morgan et al. [26] for Mean and Range of Trabecular Bone Density

	Morgan et al. Study	Earth Baseline
Density (g/cm^3)	0.56 (0.26 – 0.75)	0.501

3.2 Space Simulation Validation

The space simulation was validated by comparing its results for percent change per month of density to those of Lang et al [5]. Figure 8 shows a contour plot of density after the space simulation, representing the state of the bone immediately upon return to Earth from spaceflight.

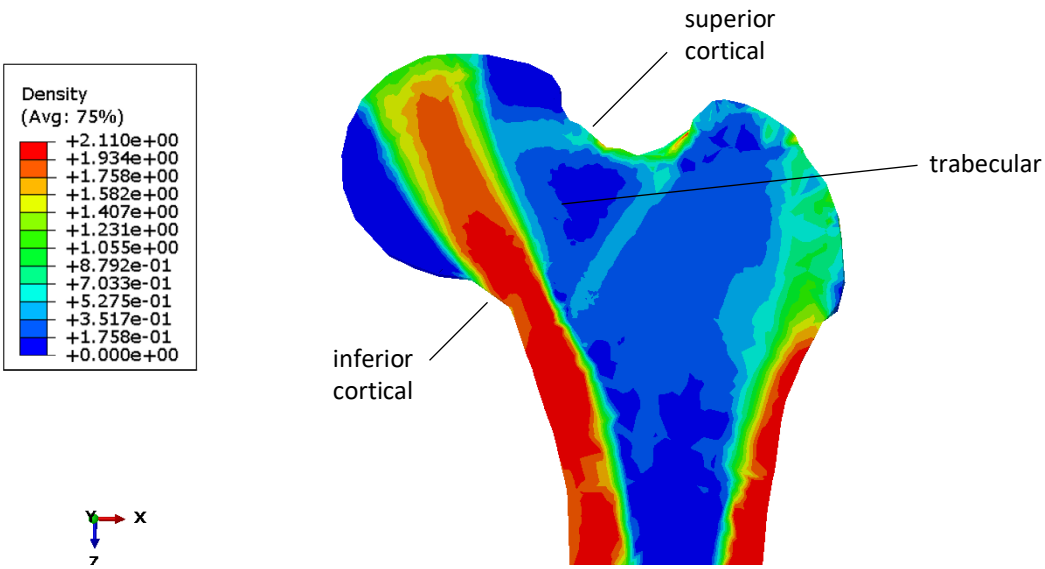

Figure 8. Contour Plot of Density (g/cm3) after Space Simulation

Values for the percent change per month of vBMD were obtained from the model for cortical bone in the inferior and superior neck regions and trabecular bone. The model results for both types of bone (0.29% decrease for the cortical region and 3.02% decrease for trabecular bone) are very accurate in comparison to those of Lang et al. [5] (0.30% decrease for cortical and 2.70% decrease for trabecular), and are within the standard deviations, as shown in Table 4. This serves to validate the space simulation.

Table 4. Comparison of Space Model Values to Lang et al. [5] Values for Percent Decrease per Month of Density (standard deviation in parenthesis)

		Lang et al.	Space Model
Density Percent Change per Month	Cortical Neck	0.30 (0.6)	0.29
	Trabecular Neck	2.70 (1.9)	3.02

3.3 Postflight Simulation

The postflight simulation was run for twelve months with the original joint force and muscle loading scheme for the Earth baseline model. Data were collected every 30 days postflight for damage per bone tissue area, BMU activation frequency, and density for each region of cortical bone in the inferior and superior neck, and trabecular bone. The entirety of this data can be found in Appendix C.

3.3.1 Postflight: Cortical Bone Regions

To condense the data and better visualize the trends, the values were averaged for the elements across each region of cortical bone. These are shown in Table 5 for cortical bone, inferior and superior neck regions combined, along with the averages from the Earth baseline and space simulations.

Table 5. Earth, Space, and Postflight Data for Damage, Activation Frequency, and Density of Cortical Bone (Inferior and Superior Neck Regions)

Time	Damage (mm/mm^2)	Activation Frequency ($BMUs/mm^2/day$)	Density (g/cm^3)
Earth Baseline	0.0406	0.0198	1.3962
Space	0.0448	0.0185	1.3723
1M PF	0.0469	0.0059	1.3857
2M PF	0.0477	0.0202	1.3953
3M PF	0.0498	0.0092	1.3890
4M PF	0.0516	0.0102	1.3899
5M PF	0.0530	0.0125	1.3913
6M PF	0.0548	0.0097	1.3893
7M PF	0.0565	0.0101	1.3894
8M PF	0.0580	0.0102	1.3893
9M PF	0.0596	0.0095	1.3885
10M PF	0.0612	0.0095	1.3883
11M PF	0.0628	0.0093	1.3880
12M PF	0.0644	0.0091	1.3875

3.3.1.1 Postflight: Damage in Cortical Bone of the Inferior and Superior Neck

The data were then plotted to better visualize and understand the behavior of damage, activation frequency, and density over time. After spaceflight, damage in cortical bone (Figure 9) increased by nearly 10%. Upon return to earth, it continued to increase over the 12 months until reaching an overall increase of 60% from the Earth baseline model, indicating a possible increase in fracture risk in these regions.

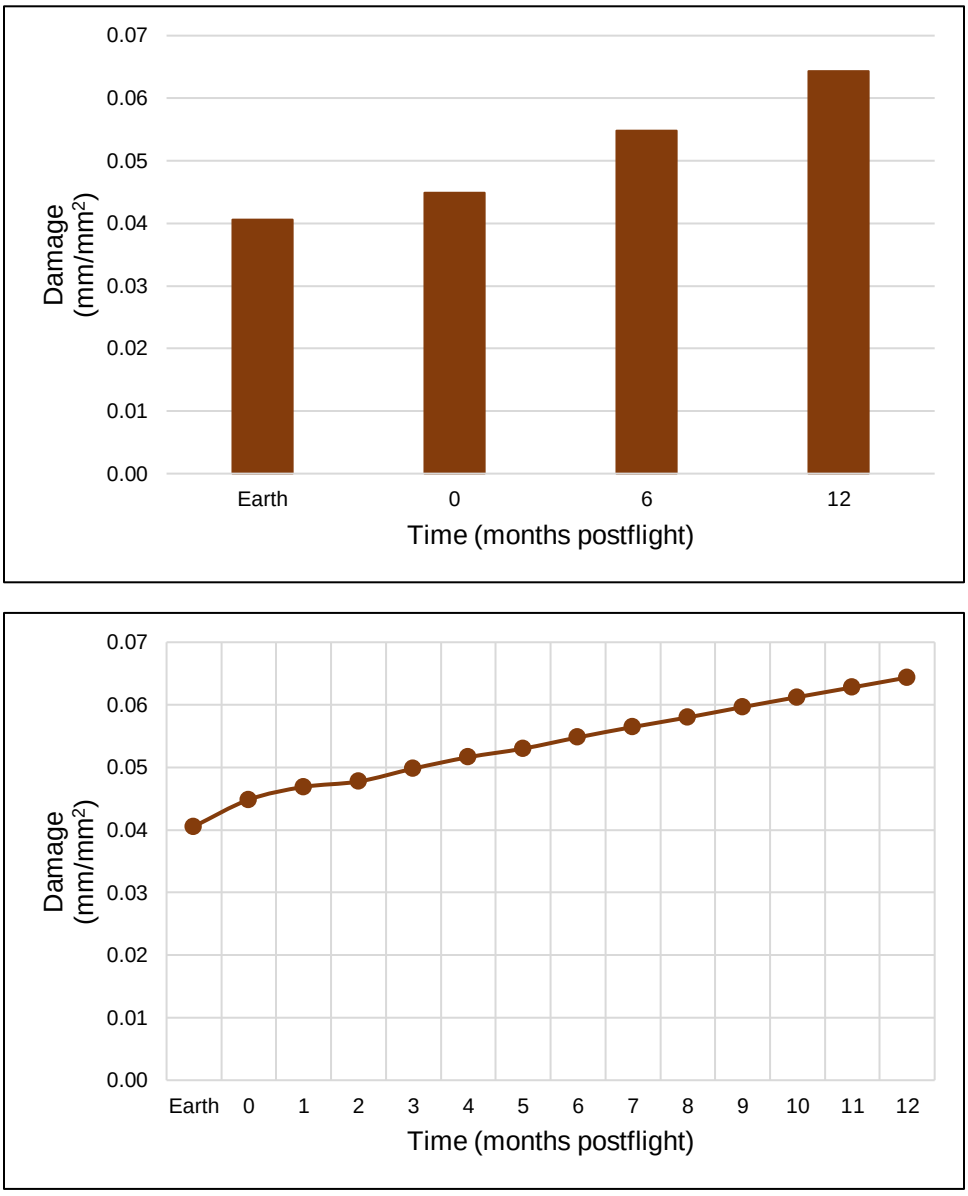

Figure 9. Damage vs. Time of Cortical Bone (Inferior and Superior Neck Regions Combined)

3.3.1.2 Postflight: BMU Activation Frequency in the Cortical Bone of the Inferior and Superior Neck

After the six months in space, the activation frequency of cortical bone (Figure 10) had decreased slightly by approximately 6%. Immediately after spaceflight, it significantly decreased then increased back to near Earth baseline levels, before dropping again. It then oscillated sharply for five months before stabilizing and steadily decreasing for the remainder of the twelve months. Overall, activation frequency decreased by nearly 55%.

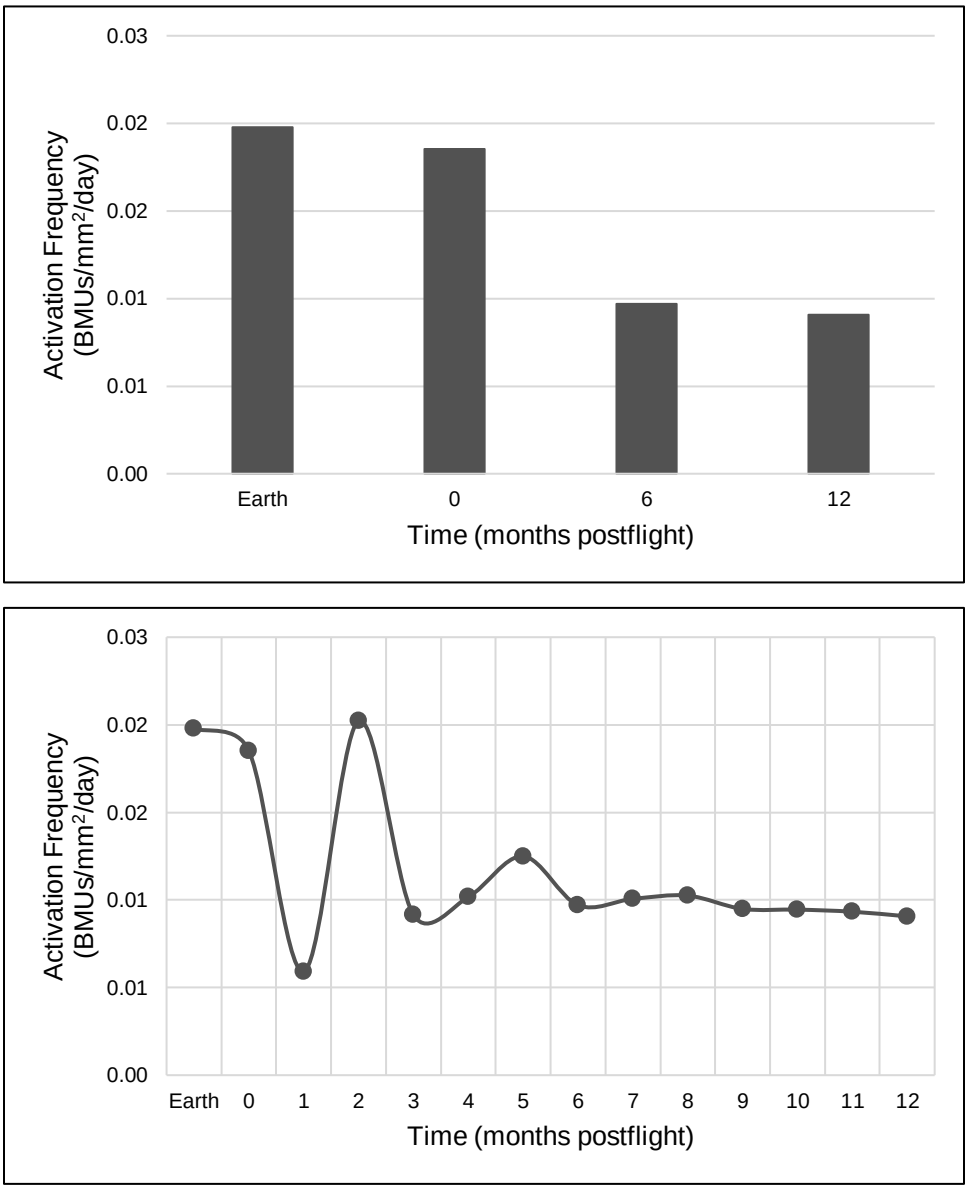

Figure 10. Activation Frequency vs. Time for Cortical Bone (Inferior and Superior Neck Regions Combined)

3.3.1.3 Postflight: Density in the Cortical Bone of the Inferior and Superior Neck

The density of cortical bone decreased by approximately 2% after six months of spaceflight (Figure 11). After returning to the Earth, density increased to a value slightly less than that of preflight, and then remained at an equilibrium for the remainder of the simulation. Overall, cortical density decreased by 0.6% in the inferior and superior neck combined.

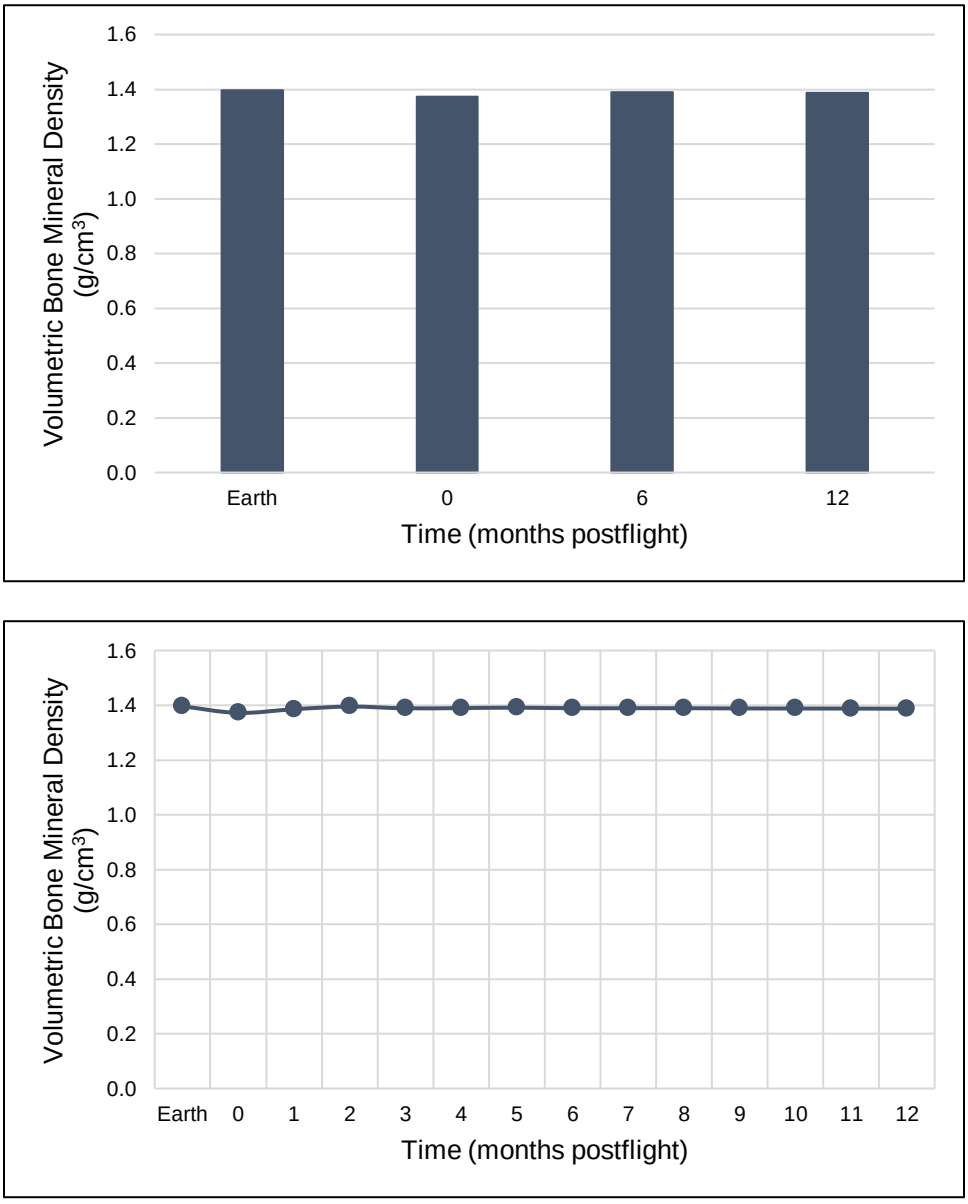

Figure 11. Density vs. Time for Cortical Bone (Inferior and Superior Regions Combined)

3.3.2 Postflight: Trabecular Bone Region

The same data were collected for the damage, activation frequency, and density of trabecular bone in the femoral neck from the Earth baseline, space, and postflight simulations. This is shown below in Table 6, and plotted against time in Figures 12 – 14.

Table 6. Earth, Space, and Postflight Data for Density, Damage, and Activation Frequency of Trabecular Bone in the Femoral Neck

Time	Damage (mm/mm^2)	Activation Frequency ($BMUs/mm^2/day$)	Density (g/cm^3)
Earth Baseline	0.0213	0.0743	0.5015
Space	0.0302	0.0630	0.4106
1M PF	0.0327	0.0119	0.4493
2M PF	0.0330	0.0442	0.4847
3M PF	0.0362	0.0264	0.4731
4M PF	0.0391	0.0222	0.4702
5M PF	0.0415	0.0276	0.4755
6M PF	0.0445	0.0235	0.4725
7M PF	0.0473	0.0218	0.4712
8M PF	0.0502	0.0222	0.4716
9M PF	0.0531	0.0208	0.4703
10M PF	0.0560	0.0199	0.4694
11M PF	0.0589	0.0195	0.4688
12M PF	0.0618	0.0187	0.4678

3.3.2.1 Postflight: Damage in the Trabecular Region

The damage in trabecular bone of the femoral neck increased by nearly 42% after spaceflight, and continued to increase significantly on Earth (Figure 12). By the end of the twelve month, postflight simulation, damage increased significantly with an overall increase of 190% from the Earth baseline model, indicating a possible increase in fracture risk in this region.

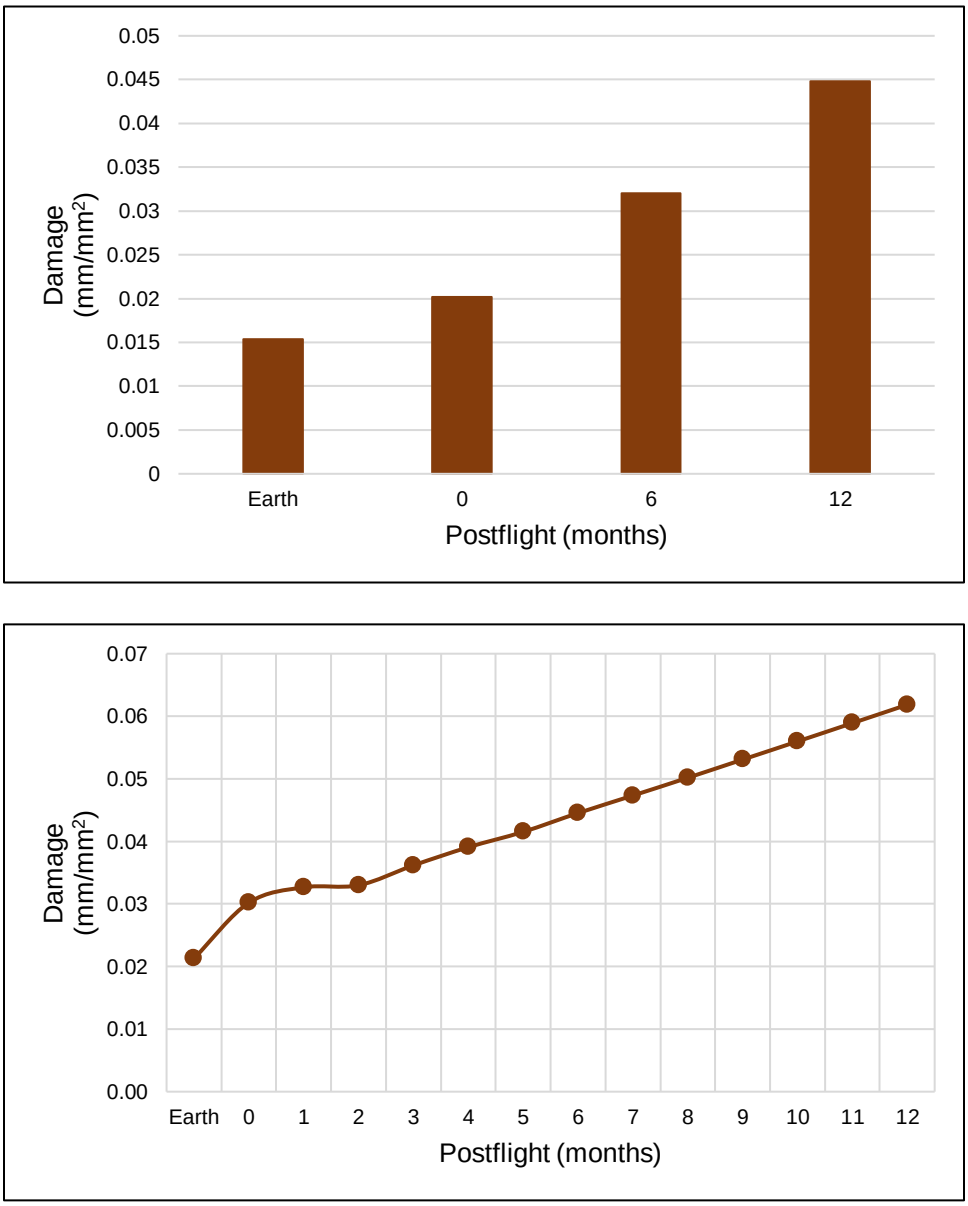

Figure 12. Damage vs. Time for Trabecular Bone

3.3.2.2 Postflight: BMU Activation Frequency in the Trabecular Region

The activation frequency of trabecular bone decreased after six months in space by 15% (Figure 13). Immediately upon return to Earth it decreased again before rising slightly, oscillating sharply for several months, and then steadily decreasing. Overall, activation frequency decreased by approximately 75%.

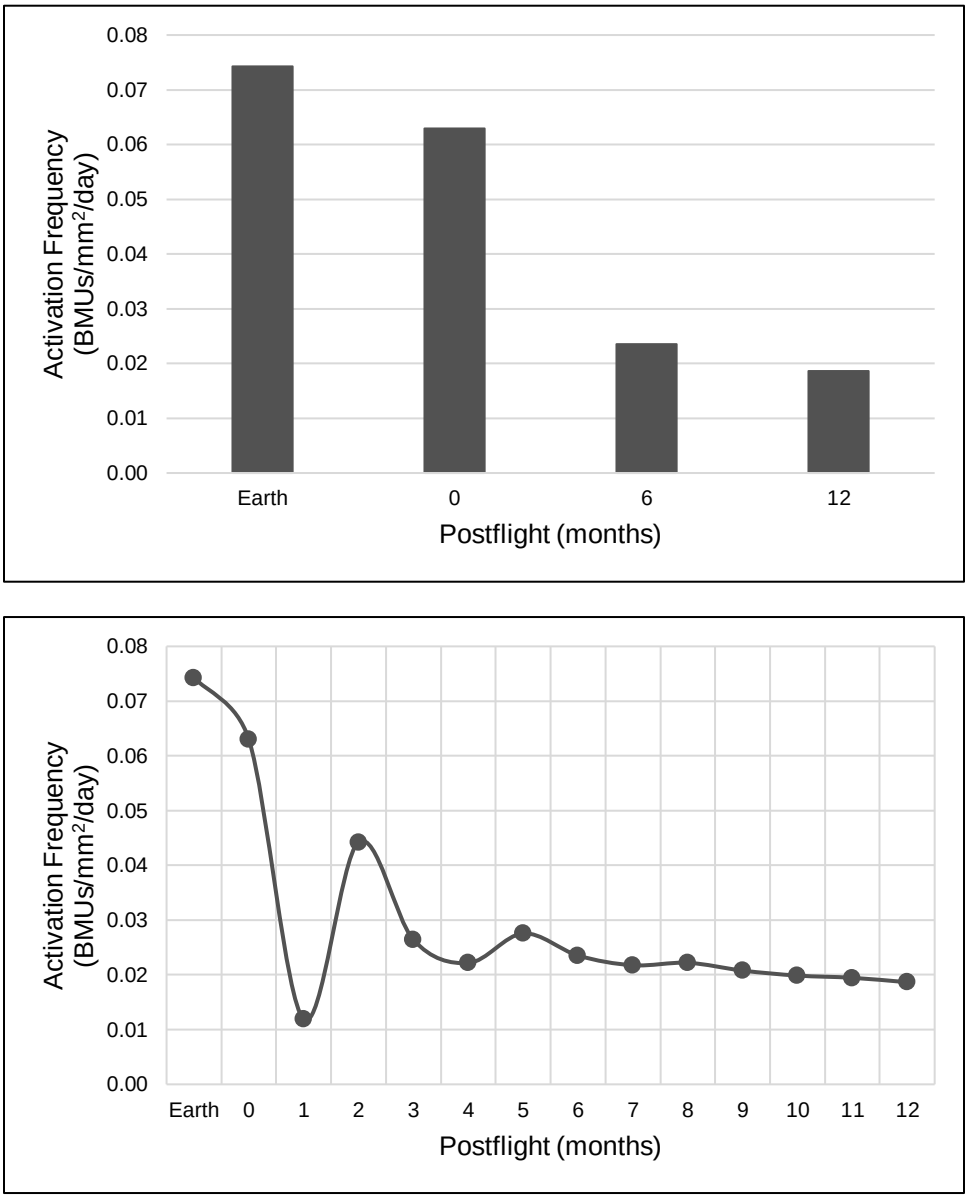

Figure 13. Activation Frequency vs. Time for Trabecular Bone

3.3.2.3 Postflight: Density in the Trabecular Region

After six months of spaceflight, the density of trabecular bone decreased by approximately 18% (Figure 14). After returning to Earth, density increased immediately before staying at a steady state for the remainder of the simulation. After the twelve months, it had decreased overall by 4%.

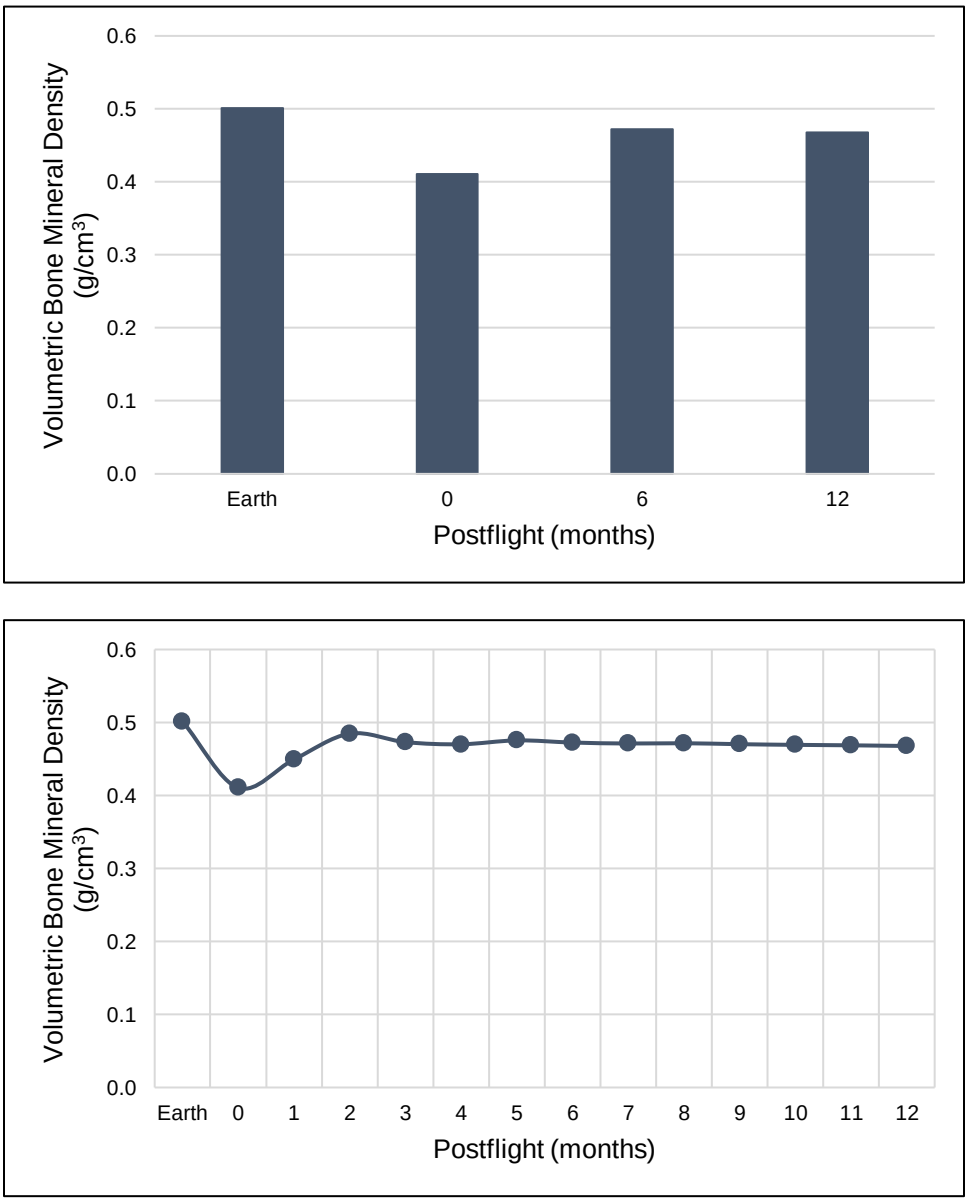

Figure 14. Volumetric Bone Mineral Density vs. Time for Trabecular Bone

4. DISCUSSION

The objective of this study was to use finite element modeling to investigate the effects of spaceflight on the human femur – the bone which experiences the most significant effects. This was done by simulating the environments of Earth preflight, a six-month mission on the International Space Station, and one year on Earth postflight. Data were collected from each simulation for damage per bone tissue area, BMU activation frequency, and density. This data was then used to provide evidence for fracture risk in the femoral neck, and to predict when it is most prominent upon return to Earth.

4.1 Earth Baseline Simulation and Validation

The Earth baseline simulation was used to bring the femur to the equilibrium conditions of a skeletally mature, active human. This was achieved by placing everyday walking and stairclimbing loads at a rate of 10,000 steps per day. The simulation was validated against an experimental study by Deuel [21], which measured surface strain in four regions of cadaveric femurs. Averaged values for the four regions were taken from the model and compared to Deuel's values. All values were within two standard deviations of the experimental results, thus validating the Earth baseline simulation. Differences in values could be attributed to the probability that the simulation used a higher number of loading cycles, thus adapting the femur to higher strain levels in these four regions.

The simulation was further validated using its results for density of cortical bone in the inferior neck region and trabecular bone. For cortical bone, a study by Yeni et al. [30] was used which measured density in the femoral neck of cadavers. For trabecular bone, a study by Morgan et al. [26] was used that measured the density of trabecular bone in the proximal femur. The results from the simulation for each bone type were extremely accurate and well within the range of measured values of their respective studies.

4.2 Space Simulation and Validation

The space simulation introduced the environment of microgravity in spaceflight by reducing the magnitude of the everyday joint and muscle loads. This was done for six months to mimic the average length of missions to the ISS. The number of loading cycles was not reduced to compensate for the considerable amounts of exercise performed by astronauts in flight. The simulation was validated using its results for percent change per month of density in both cortical (inferior and superior neck regions combined) and trabecular bone. They were compared to the results of a study by Lang et al. [5], which measured the percent change per month for both types of bone for a six-month mission in space. The density values from the simulation were very accurate in comparison to those by Lang et al. and well within the range of values measured in that study.

4.3 Postflight Simulation

The postflight simulation was used to return the model to Earth conditions with daily loads scaled back to their original values. This was done for twelve months to provide the most comprehensive understanding of changes in bone immediately after flight and in the following year. After spending six months on the ISS and having returned to Earth for twelve months, the proximal femur demonstrated large changes across damage, BMU activation frequency, and density in both cortical and trabecular bone.

Cortical bone in the femoral neck, inferior and superior regions combined, experienced significant changes in damage as a result of spaceflight. After six months on the ISS, damage increased drastically and continued to increase after returning to Earth, without reaching an equilibrium. This resulted in a 59% increase between the preflight and end of postflight simulation values. This increase in damage occurred because the microgravity environment of space resulted in reduced loading and signaled a state of disuse, lowering bone remodeling levels as seen by the sharp initial decrease in BMU activation frequency. Although less damage was being formed due to the reduced loading, even less damage was removed due to the decreased activity of the cells, increasing the rate of accretion. Damage accumulates because the activation of remodeling cells cannot keep up with the amount of damage being formed, and are simultaneously not removing

damage quickly enough. Gardina [19], who also implemented the algorithm by Hazelwood et al. [9], modeled a similar significant increase in damage, which continued to increase after returning to Earth. His model also predicted that damage would require approximately 15 years to reach a steady value. Therefore, it is expected that damage would not reach equilibrium in the one-year, postflight simulation.

The greatest magnitude of damage in cortical bone was found in the inferior neck region. However, the greatest increase in damage after flight and return to Earth was in the superior neck region where damage increased approximately 198%. Both cases contribute significantly to bone fragility, increasing fracture risk in the femoral neck. Large amounts of bone damage decrease resistance to fracture and high rates of damage accumulation diminish the toughness of bone and make it more susceptible to fracture [31]. While the exact amount of damage required to result in fracture is unknown, it is reasonable to deduce that higher magnitudes and increases of damage will contribute to the susceptibility of fracture. This confirms that the femoral neck, both the inferior and superior neck regions, are very prone to fracture. Because damage will probably continue to accumulate without nearing equilibrium for so long, it is not possible to determine exactly when fracture risk is most prominent.

BMU activation frequency, a function of disuse and damage, exhibited the greatest changes in cortical bone in response to spaceflight and particularly upon return to Earth. After the six months in space, activation frequency decreased slightly from its preflight value. This is to be expected, as the microgravity environment of space results in decreased everyday loads, simulating a state of disuse. When back on Earth, it decreased much more significantly and then oscillated sharply for several months before stabilizing, but never reaching a true equilibrium. At the end of the postflight simulation, activation frequency exhibited an overall decrease of 54%.

As predicted by Hazelwood et al. [9], activation frequency oscillates greatly when loads are reduced, and falls to standard values when they are returned to normal. These oscillations are even more significant and greater in duration when disuse is more severe. This transient behavior as a result of disuse has been documented in several other studies. An experiment by Uhthoff and Jaworski [32] monitored bone loss in dogs whose right limb was immobilized in a flexed position

for varying periods of time up to forty weeks. Radiographs were taken to monitor bone mass over the course of eight weeks and data were collected for bone area and total active surface (resorption and formation surfaces combined). The total active surface, representing BMU activation frequency, exhibited oscillatory behavior that eventually stabilized and decreased. Another experiment by Hardt [33] studied femoral bone response to disuse in white male rabbits whose limbs were immobilized using calcaneal tenotomy. After varying periods of immobilization of up to 18 days, the rabbits were euthanized and their femurs demineralized and analyzed. An oscillatory pattern similar to that of BMU activation frequency was exhibited by the bone mineral content of the rabbits' femora. This is representative of the bone metabolic activity, which relates to the activity of BMUs.

Although this oscillatory response is supported by these studies and more, the ultimate cause remains unknown. However, it is likely due to the fact that although damage initiates the activation of BMU's, there is a time lag in the remodeling process. When cavities are not being refilled as fast as they are being resorbed, they will add to temporal porosity. In this time, BMU activation frequency oscillates, attempting to achieve a homeostatic equilibrium in bone mass. If loading conditions are severe enough, oscillations will be sharper and the time lag will be prolonged, requiring more time for values to stabilize.

The density of cortical bone overall experienced an overall decrease of 0.5% in density as a result of BMU activation frequency. Because bone loss is the primary effect of long duration spaceflight, it is expected that density will decrease [34]. This is a result of the remodeling process prompted by disuse, as remodeling increases porosity of bone and decreases density. In the absence or decrease of loads, there is an increase of resorbing and a decrease in refilling BMUs [35]. Porosity is calculated at each step in time of the simulation, and is based on the temporal and geometric characteristics of these BMUs [9]. Therefore, when BMU activation frequency increases in response to disuse and damage, porosity also increases and density decreases.

This decrease in density was observed in both regions of cortical bone of the femoral neck. However, it was smaller in magnitude in the inferior region (0.16%) where density is the highest, and larger (4.5%) in the superior neck region where it is the lowest [36]. In the inferior neck region,

dense cortical bone provides a rigid lining that protects the proximal femur. A thinning of this lining as a result of bone loss, regardless of magnitude, can be harmful. It is also of concern in the superior neck region, as large increases over small amounts of time will rapidly decrease bone strength. The study by Keyek et al. [18], which also used finite element modeling to observe the effects of spaceflight on bone, also found substantial losses in bone density and suggested a resulting decrease in bone strength after long-duration spaceflight.

The greatest decline in cortical bone density (inferior and superior neck regions combined) was seen immediately after spaceflight. After returning to Earth, density increased and then oscillated slightly for five months before levelling off at a value less than that of pre-flight. In this time, the entire remodeling cycle, which typically requires three to four months to complete, occurred and returned density to a stable value. The final value of density was less than that of preflight, suggesting that mass does not completely recover over a one-year period after returning to Earth. In his model, Gardina [5] also found bone density to decrease after flight, but recover slightly after returning to Earth. This behavior of density is supported by a study from Vico et al. [37] who measured bone density of weight-bearing bones in cosmonauts who traveled to space for two or six-month missions. Measurements were taken prior to flight, immediately after flight, and six months postflight. It was found that density did not return to preflight values for most of the cosmonauts. This loss of mass affects bone strength indefinitely, contributing to the risk of fracture.

Similar to damage, it is unclear as to what extent density contributes to fracture risk. It is certain however, that loss of bone mass, as captured by density decreases, is a risk factor for fracture [38]. Even if a decrease in density is not severe enough to cause fracture immediately upon return from flight, it is likely to lead to several health complications later in life [18]. Bone loss will accelerate the onset of osteoporosis, increase its severity, and add to fall risk due to bone fragility. This will increase the likelihood of age-related hip fractures in astronauts, long after their time in space.

In the region of trabecular bone, spaceflight followed by a return to Earth for 12 months caused an extremely high increase of 190% in damage. Like cortical bone, damage continued to increase back on Earth, and did not reach an equilibrium, as it was expected that damage levels

would not stabilize within the duration of the postflight simulation. By the end of the twelve months, the magnitude of damage had nearly tripled from its spaceflight value. While cortical and trabecular bone in the neck completed the postflight simulation with similar damage values, the initial, preflight value for the trabecular region was less than that of cortical bone (inferior and superior neck combined). This is because damage represents damage per area of bone tissue. Trabecular bone is far less dense and contains a much smaller amount of tissue per total bone area, so this value is naturally smaller. Its high porosity makes trabecular bone much more susceptible to damage.

In the overall proximal femur, the greatest increase in damage over time was in cortical bone in the superior region of the neck where values increased by 198%. And while damage per bone tissue was similar in all areas, the greatest magnitude of damage per total bone volume was seen in cortical bone in the inferior region of the neck. This confirms that in the proximal femur, fracture risk is likely to be extremely prominent in the inferior and superior regions of the femoral neck. This is supported by the fact that naturally, the neck is most prone to fracture due to old age and medical complications such as osteoporosis [39]. While damage typically only increases the risk, it could in some cases lead to complete fracture. Damage is a measure of crack length per tissue area, and such cracks could be accelerated by the energy of a fall and increase stress [40]. If this stress becomes too great, it is likely that the bone's toughness will not be able to withstand complete fracture.

BMU activation frequency in trabecular bone exhibited the same pattern as in cortical bone, decreasing slightly after spaceflight, and then drastically in the first month postflight. Over the next five months it oscillated sharply before stabilizing, but not reaching a true, steady value. While the behavior of activation frequency matched that of cortical bone, the magnitude was much greater with an overall decrease of 75%. The oscillations were much sharper as the peak level of activation frequency was four times that of cortical bone. This is a direct result of the larger increases in damage compared to cortical bone in the neck (190% to 59%). A greater magnitude of damage will activate more BMUs in the same amount of time, increasing the rate of resorbing BMUs and decreasing refilling BMUS. Additionally, because trabecular bone is more porous it holds a lot of bone marrow which contains bone cells that are readily available to be activated.

The density of trabecular bone decreased significantly as a result of the high accretion rate of damage and increased rate of resorbing BMUs. As with the other two variables, trabecular bone density exhibited similar behavior to that of cortical bone, but on a much larger scale. After six months of spaceflight, density experienced a large decrease. In the first two months back on Earth, density increased to a value just slightly less than the preflight value, oscillated slightly for a few months, and then maintained a steady value for the remainder of the twelve months. In this time the remodeling cycle was completed, allowing density to reach an equilibrium. This resulted in a decrease of approximately 7% between preflight and 12 months postflight.

The larger changes in density are also attributed to the fact that trabecular bone is far more porous than cortical. This results in the low initial value of damage per bone tissue, high damage accretion rate, and consequently the high BMU activation frequency. In their study on long-duration spaceflight, Lang et al. [5] also found density to decrease in the proximal femur in both cortical and trabecular bone, with larger percent losses in the trabecular region. Because trabecular bone has less mass to begin with, this decrease in density can be especially detrimental. The lowest value of density occurred two months after space flight, and while it is not possible to know if this is enough to cause an immediate fracture risk, the overall loss of bone may add to complications later in life.

4.4 Limitations

The algorithm by Hazelwood et al. [9] and finite element model by Deuel [21] were successful in this thesis in simulating the environments on Earth and space and delivering interpretable results. By increasing the amount of loading cycles to match the activity of an astronaut, and decreasing the magnitudes of loads to mimic spaceflight, an accurate study was produced that provided evidence for fracture risk in the human femur. There were, however, several limitations in the model and simulations that should be considered.

The finite element model of the femur was developed from computed tomography (CT) scans of a femur obtained from an adult, male cadaver weighing 188 pounds. The results from the simulations therefore are representative of a male, and would not fully match those of a female.

This would most likely be due to increased levels of estrogen in females, as the hormone plays a key role in regulating bone growth and remodeling [41]. Higher levels of estrogen lower the disuse and overload threshold to which BMUs are activated in response to [42]. The geometry of bone also differs between males and females, as shown in a study by Kaji et al. that used peripheral quantitative computed tomography (pQCT) to compare differences in bone between genders [43]. Kaji et al. found bone geometry and bone strength index (polar strength strain index (SSIp)), a surrogate measure of strength, to be higher in males. In studying age-related changes, they also found that females lost more density in cortical bone, and similar amounts in trabecular bone. These differences suggest that the response of bone shown in this thesis may differ for that of a female astronaut. Additionally, the weight of the individual from the model, though not exceeding current physical requirements, is likely more than that of the typical astronaut. A lower weight value would decrease the magnitudes of the joint and muscle loads and the results would differ.

The bone remodeling algorithm and its equations also pose several limitations. The constants and initial values used in calculations for the algorithm were based on the activity and characteristics of the average adult. If values were based on an astronaut, who is much more active, they would differ, perhaps significantly. Another factor of the algorithm that should be considered is the amount of loading cycles used in the space simulation. This value was kept at 5,000 cycles (10,000 steps per day) to represent the substantial amount of activity done in space through the typical exercise regimen. In-flight exercises and their associated loads were not modeled in an effort to simplify the model. This would be extremely useful to implement in future studies in order to produce a more realistic simulation and accurate results for changes in properties.

Another limitation that should be accounted for is the lack of data pertaining to damage and fracture risk. While studies have confirmed that damage is a contributor, they have not been able to quantify how much damage is associated with fracture risk. Furthermore, as shown by the results of this study, damage takes many years to stop decreasing and stabilize after returning to Earth, making it difficult to predict the behavior of damage beyond the length of the simulations. Instead, this thesis focused on the percent increases in damage and the reasoning behind high accumulation rates.

5. CONCLUSION

Spending six months in the microgravity environment of the International Space Station had a significant effect on cortical bone in the femoral neck, both in the inferior and superior regions, as well as on trabecular bone in the neck. The decrease in loads in space signaled a state of disuse that lowered bone remodeling levels. This in turn increased damage, activation frequency, and porosity, causing both types of bone to lose mass and decrease in density. The greatest increase in damage was seen in the superior region of the femoral neck, and the greatest magnitude in the inferior region of the neck. The largest percent decrease in density occurred in trabecular bone, followed by the cortical bone in superior neck region, and the inferior neck region. These changes confirm that the femoral neck is highly prone to fracture risk as a result of spaceflight.

The timeline of spaceflight and fracture risk is still unknown, but will become clear when more data are collected and uncertainty is reduced [38]. Damage did not reach an equilibrium in the one-year, postflight simulation and likely will not for many years. After its lowest value two months after returning to Earth, a substantial amount of density was recovered after several bone remodeling cycles were completed. It is known however, that bone density and bone strength do not recover from these effects in the immediate year upon returning to Earth [18]. Although this decrease in density is likely insufficient to increase fracture risk immediately upon return to Earth, it may contribute to complications later in life such as early onset osteoporosis and fall risk [5] [34]. While the bone loss that occurs during the typical six-month mission does not create an unacceptable risk during flight, it is clear that there is a correlation between time in space and bone loss [38] [44].

Consequently, missions lasting longer than six months could impose a more serious risk to fracture. Additionally, the results from this study support the claim that the current, in-flight exercise regime may not be effective enough in maintaining bone mass in lower limbs such as the femur [27]. With longer missions lasting one to three years planned for the future, these results suggest that the fitness of crewmembers will need improvement [15].

REFERENCES

[1] LeBlanc, A., et al. “Bone Mineral and Lean Tissue Loss after Long Duration Space Flight.” *J Musculoskel Neuron Interact*, vol. 1, no. 2, 2000, pp. 157–160.

[2] Coulombe, Jennifer C., et al. “Spaceflight-Induced Bone Tissue Changes That Affect Bone Quality and Increase Fracture Risk.” *Current Osteoporosis Reports*, vol. 18, no. 1, 2020, pp. 1–12., doi:10.1007/s11914-019-00540-y.

[3] Johnston, C. C., and C. W. Slemenda. “Peak Bone Mass, Bone Loss and Risk of Fracture.” *Osteoporosis International*, vol. 4, no. S1, 1994, doi:10.1007/bf01623435.

[4] Burr, David. “Microdamage and Bone Strength.” *Osteoporosis International*, vol. 14, 2003, pp. 67–72., doi:10.1007/s00198-003-1476-2.

[5] Lang, T., LeBlanc, A., Evans, H., Lu, Y., Genant, H. and Yu, A. (2004), Cortical and Trabecular Bone Mineral Loss From the Spine and Hip in Long-Duration Spaceflight. J Bone Miner Res, 19: 1006-1012. doi:10.1359/JBMR.040307

[6] Lang, Thomas F, et al. “Adaptation of the Proximal Femur to Skeletal Reloading After Long-Duration Spaceflight.” *Journal of Bone and Mineral Research*, vol. 21, no. 8, 2006, pp. 1224–1230., doi:10.1359/jbmr.060509.

[7] LeBlanc, A. D., et al. “Skeletal Responses to Space Flight and the Bed Rest Analog: A Review.” *J Musculoskelet Neuronal Interact*, vol. 7, no. 1, Oct. 2005, pp. 33–47.

[8] Hadjidakis, D. J., and I. I. Androulakis. “Bone Remodeling.” *Annals of the New York Academy of Sciences*, vol. 1092, no. 1, 2006, pp. 385–396., doi:10.1196/annals.1365.035.

[9] Hazelwood, Scott J, et al. “A Mechanistic Model for Internal Bone Remodeling Exhibits Different Dynamic Responses in Disuse and Overload.” *Journal of Biomechanics*, vol. 34, no. 3, Mar. 2001, pp. 299–308., doi:10.1016/s0021-9290(00)00221-9.

[10] Raggatt, Liza J., and Nicola C. Partridge. “Cellular and Molecular Mechanisms of Bone Remodeling.” *Journal of Biological Chemistry*, vol. 285, no. 33, 2010, pp. 25103–25108., doi:10.1074/jbc.r109.041087.

[11] Eriksen, Erik Fink. “Cellular Mechanisms of Bone Remodeling.” *Reviews in Endocrine and Metabolic Disorders*, vol. 11, no. 4, 2010, pp. 219–227., doi:10.1007/s11154-010-9153-1.

[12] Dunbar, Brian. “What Is Microgravity?” *NASA*, NASA, 13 May 2015, www.nasa.gov/centers/glenn/shuttlestation/station/microgex.html.

[13] Dunbar, Brian. “What Is Microgravity?” *NASA*, NASA, 16 June 2015, www.nasa.gov/audience/forstudents/5-8/features/nasa-knows/what-is-microgravity-58.html.

[14] Rogers, Melissa J. B., et al. *Microgravity: a Teacher's Guide with Activities in Science, Mathematics, and Technology*. National Aeronautics and Space Administration, Office of Life and Microgravity Sciences and Applications, Microgravity Research Division, 1997.

[15] Trappe, Scott, et al. “Exercise in Space: Human Skeletal Muscle after 6 Months Aboard the International Space Station.” *Journal of Applied Physiology*, vol. 106, no. 4, 1 Apr. 2009, pp. 1159–1168., doi:10.1152/japplphysiol.91578.2008.

[16] Cavanagh, Peter R., et al. “Exercise and Pharmological Countermeasures for Bone Loss During Long-Duration Space Flight.” *American Society for Graviational and Space Biology*, vol. 18, no. 2, July 2005, pp. 39–58.

[17] Iwamoto, Jun, et al. “Interventions to Prevent Bone Loss in Astronauts during Space Flight.” *The Keio Journal of Medicine*, vol. 54, no. 2, 2005, pp. 55–59., doi:10.2302/kjm.54.55.

[18] Keyak, J.h., et al. “Reduction in Proximal Femoral Strength Due to Long-Duration Spaceflight.” *Bone*, vol. 44, no. 3, Mar. 2009, pp. 449–453., doi:10.1016/j.bone.2008.11.014.

[19] Gardina, Christopher. “Bone Mass Preservation and Fracture Risk Assessment with Bisphosphonate Therapy During Spacellight.” *California Polytechnic State University, San Luis Obispo*, 2008.

[20] Garcia, Mark. “Past Expeditions.” *NASA*, NASA, 6 Feb. 2020, www.nasa.gov/mission_pages/station/expeditions/past.html.

[21] Deuel, Christopher Robert. “Development of an Adaptive 3-D Model of the Human Femur to Simulate Bone Remodeling Following Hip Resurfacing and Total Hip Arthroplasties.” *University of California Davis*, 2007.

[22] Viceconti, Marco, et al. “A Comparative Study on Different Methods of Automatic Mesh Generation of Human Femurs.” *Medical Engineering & Physics*, vol. 20, no. 1, Apr. 1998, pp. 1–10., doi:10.1016/s1350-4533(97)00049-0.

[23] Whalen, R.t., et al. “Influence of Physical Activity on the Regulation of Bone Density.” *Journal of Biomechanics*, vol. 21, no. 10, 1988, pp. 825–837., doi:10.1016/0021-9290(88)90015-2.

[24] Mcleish, R.d., and J. Charnley. “Abduction Forces in the One-Legged Stance.” *Journal of Biomechanics*, vol. 3, no. 2, Mar. 1970, pp. 191–209., doi:10.1016/0021-9290(70)90006-0.

[25] Bergmann, G, et al. “Hip Contact Forces and Gait Patterns from Routine Activities.” *Journal of Biomechanics*, vol. 34, no. 7, July 2001, pp. 859–871., doi:10.1016/s0021-9290(01)00040-9.

[26] Morgan, Elise F., et al. “Trabecular Bone Modulus–Density Relationships Depend on Anatomic Site.” *Journal of Biomechanics*, vol. 36, no. 7, July 2003, pp. 897–904., doi:10.1016/s0021-9290(03)00071-x.

[27] Blodgett, Rachael. “Frequently Asked Questions.” *NASA*, NASA, 16 Jan. 2018, www.nasa.gov/feature/frequently-asked-questions-0/.

[28] Tudor-Locke, Catrine, and David R Bassett. “How Many Steps/Day Are Enough?” *Sports Medicine*, vol. 34, no. 1, Jan. 2004, pp. 1–8., doi:10.2165/00007256-200434010-00001.

[29] Deuel, C. R., et al. “Alterations in Femoral Strain Following Hip Resurfacing and Total Hip Replacement.” *The Journal of Bone and Joint Surgery. British Volume*, 91-B, no. 1, 1 Jan. 2009, pp. 124–130., doi:10.1302/0301-620x.91b1.20789.

[30] Yeni, Y.n., and T.l. Norman. “Fracture Toughness of Human Femoral Neck: Effect of Microstructure, Composition, and Age.” *Bone*, vol. 26, no. 5, May 2000, pp. 499–504., doi:10.1016/s8756-3282(00)00258-1.

[31] Schaffler, M.b., et al. “Aging and Matrix Microdamage Accumulation in Human Compact Bone.” Bone, vol. 17, no. 6, Dec. 1995, pp. 521–525., doi:10.1016/8756-3282(95)00370-3.

[32] Uhthoff, Hk, and Zf Jaworski. “Bone Loss in Response to Long-Term Immobilisation.” *The Journal of Bone and Joint Surgery. British Volume*, 60-B, no. 3, Aug. 1978, pp. 420–429., doi:10.1302/0301-620x.60b3.681422.

[33] Hardt, Alfred B. “Early Metabolic Responses of Bone to Immobilization.” *The Journal of Bone & Joint Surgery*, vol. 54, no. 1, Jan. 1972, pp. 119–124., doi:10.2106/00004623-197254010-00011.

[34] Lang, Thomas F. 4th ed., vol. 6, J Musculoskelet Neuronal Interact, 2006, pp. 319–321, *What Do We Know about Fracture Risk in Long-Duration Spaceflight?*

[35] Swaffield, Thomas P., et al. “Fracture Risk in Spaceflight and Potential Treatment Options.” *Aerospace Medicine and Human Performance*, vol. 89, no. 12, 2018, pp. 1060–1067., doi:10.3357/amhp.5007.2018.

[36] Loveridge, Nigel, et al. “Bone Mineralization Density and Femoral Neck Fragility.” *Bone*, vol. 35, no. 4, 2004, pp. 929–941., doi:10.1016/j.bone.2004.05.025.

[37] Vico, Laurence, et al. “Effects of Long-Term Microgravity Exposure on Cancellous and Cortical Weight-Bearing Bones of Cosmonauts.” *The Lancet*, vol. 355, no. 9215, 6 May 2000, pp. 1607–1611., doi:10.1016/s0140-6736(00)02217-0.

[38] Sibonga, Jean D., et al. National Aeronautics and Space Administration, 2017, *Risk of Bone Fracture Due to Spaceflight-induced Changes to Bone*, humanresearchroadmap.nasa.gov/evidence/reports/Fracture.pdf.

[39] Simon Mears, MD. *Fixing Hip Fractures*, 20 June 2017, www.hopkinsmedicine.org/gec/series/fixing_hip_fractures.

[40] Mayhew, Paul M, et al. “Relation between Age, Femoral Neck Cortical Stability, and Hip Fracture Risk.” *The Lancet*, vol. 366, no. 9480, 2005, pp. 129–135., doi:10.1016/s0140-6736(05)66870-5.

[41] Sims, N.a, et al. “Deletion of Estrogen Receptors Reveals a Regulatory Role for Estrogen Receptors-β in Bone Remodeling in Females but Not in Males.” *Bone*, vol. 30, no. 1, Jan. 2002, pp. 18–25., doi:10.1016/s8756-3282(01)00643-3.

[42] Frost, Harold M. “On Rho, a Marrow Mediator, and Estrogen: Their Roles in Bone Strength and ‘Mass’ in Human Females, Osteopenias, and Osteoporoses--Insights from a New Paradigm.” *Journal of Bone and Mineral Metabolism*, vol. 16, no. 2, 1998, pp. 113–123., doi:10.1007/s007740050035.

[43] Kaji, Hiroshi & Kosaka, Rieko & Yamauchi, Mika & Kuno, Kaoru & Chihara, Kazuo & Sugimoto, Toshitsugu. (2006). Effects of Age, Grip Strength and Smoking on Forearm Volumetric Bone Mineral Density and Bone Geometry by Peripheral Quantitative Computed Tomography: Comparisons between Female and Male. Endocrine journal. 52. 659-66. 10.1507/endocrj.52.659.

[44] Nelson, Emily S., et al. “Development and Validation of a Predictive Bone Fracture Risk Model for Astronauts.” *Annals of Biomedical Engineering*, vol. 37, no. 11, 2009, pp. 2337–2359., doi:10.1007/s10439-009-9779-x.

APPENDICES

APPENDIX A

Earth baseline simulation loads: location, direction, and magnitude

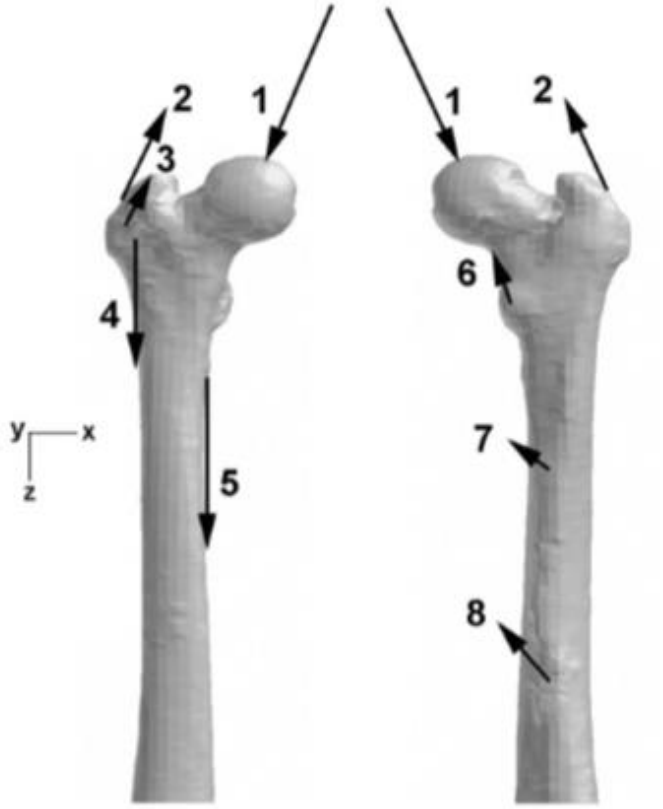

Figure 15. Joint and Muscle Forces Application Locations for Earth Baseline and Space Simulations [1. Hip joint, 2. Gluteus medius, 3. Gluteus minimus, 4. Vastus lateralis, 5. Vastus medialis, 6. Psoas, 7. Adductor brevis, 8. Adductor longus] [21]

Table 7. Earth Baseline Simulation Load Magnitudes

		Magnitude (N)		
Force	Direction	I	II	III
Hip Joint	x	3.84	3.84	3.96
	y	3.84	3.84	3.96
	z	3.84	3.84	-
Gluteus Medius	x	-11.31	-7.52	-13.89
	y	-7.38	6.18	-14.48
	z	-18.09	-20.52	-18.36
Gluteus Minimus	x	-9.21	-5.71	-9.02
	y	-6.01	4.89	-9.36
	z	-14.52	-15.84	-11.88
Vastus Medialis	x	-	-	-3.30
	y	-	-	-9.08
	z	-	-	64.40
Vastus Lateralis	x	-1.90	-	-2.38
	y	-5.23	-	-6.54
	z	34.80	-	46.40
Psoas	x	-	-2.71	-
	y	-	-2.57	-
	z	-	-5.02	-
Adductor Brevis	x	-2.73	-2.73	-2.73
	y	1.40	1.40	1.40
	z	-2.28	-2.28	-2.28
Adductor Longus	x	-5.71	-5.71	-5.71
	y	3.86	3.86	3.86
	z	-6.69	-6.69	-6.69

APPENDIX B

Space simulation loads: magnitude

Table 8. Space Simulation Load Magnitudes

		Magnitude (N)		
Force	Direction	I	II	III
Hip Joint	x	3.46	3.46	3.56
	y	3.46	3.46	3.56
	z	3.46	3.46	-
Gluteus Medius	x	-10.17	-6.77	-12.50
	y	-6.64	5.57	-13.03
	z	-16.28	-18.47	-16.52
Gluteus Minimus	x	-8.29	-5.14	-8.12
	y	-5.41	4.40	-8.42
	z	-13.07	-14.26	-10.69
Vastus Medialis	x	-	-	-2.97
	y	-	-	-8.17
	z	-	-	57.96
Vastus Lateralis	x	-1.71	-	-2.14
	y	-4.71	-	-5.89
	z	31.32	-	41.76
Psoas	x	-	-2.44	-
	y	-	-2.31	-
	z	-	-4.51	-
Adductor Brevis	x	-2.45	-2.45	-2.45
	y	1.26	1.26	1.26
	z	-2.05	-2.05	-2.05
Adductor Longus	x	-5.14	-5.14	-5.14
	y	3.47	3.47	3.47
	z	-6.02	-6.02	-6.02

APPENDIX C

All simulation data: element values for measured variables in cortical bone and trabecular bone

Table 9. Element Values for Measured Variables in Cortical Bone (Inferior and Superior Regions)

Element	Damage (mm/mm² bone tissue)	BMU Activation Frequency (BMUs/mm²/ day)	Density (g/cm³)	Element	Damage (mm/mm² bone tissue)	BMU Activation Frequency (BMUs/mm²/ day)	Density (g/cm³)
Earth Baseline Simulation							
11316	0.03299	0.00198	1.99828	**12854**	0.05693	0.00704	1.99102
11321	0.03477	0.00212	1.99715	**12857**	0.04573	0.00264	2.00173
11340	0.05347	0.00332	1.99903	**12883**	0.02829	0.00593	1.99548
11341	0.05412	0.00346	1.99663	**17222**	0.02271	0.04859	0.37857
11344	0.06291	0.00405	1.99799	**17223**	0.01520	0.06933	0.53360
11346	0.04444	0.00261	2.00012	**17226**	0.02276	0.02874	0.36410
11347	0.09170	0.00834	1.98742	**17239**	0.01830	0.03729	0.40332
11348	0.09489	0.00894	1.98607	**17241**	0.02953	0.05481	0.27772
12396	0.08133	0.00745	1.99080	**18657**	0.02266	0.07249	0.38675
12849	0.03423	0.00243	2.00044	**18660**	0.01826	0.03383	0.42029
12850	0.02737	0.00262	2.00090	**18662**	0.02101	0.02969	0.37450
12851	0.04228	0.00247	2.00104	**18663**	0.01757	0.03465	0.42639
Average	0.04056	0.01978	1.39622				
Space Simulation							
11316	0.03662	0.00329	1.99431	**12854**	0.05625	0.01235	1.98054
11321	0.03859	0.00310	1.99421	**12857**	0.04707	0.00391	1.99672
11340	0.05845	0.00371	1.99773	**12883**	0.02726	0.00886	1.98096
11341	0.05950	0.00389	1.99516	**17222**	0.03220	0.03100	0.33029
11344	0.06732	0.00444	1.99663	**17223**	0.01889	0.05017	0.45536
11346	0.04900	0.00288	1.99924	**17226**	0.03178	0.03143	0.31737
11347	0.09337	0.00828	1.98661	**17239**	0.02437	0.05329	0.34741
11348	0.09520	0.00862	1.98603	**17241**	0.04416	0.02879	0.24047
12396	0.07648	0.01016	1.98413	**18657**	0.03237	0.02463	0.33136
12849	0.03566	0.00476	1.99413	**18660**	0.02457	0.04178	0.35520
12850	0.02749	0.00620	1.99013	**18662**	0.02979	0.04799	0.32236
12851	0.04587	0.00305	1.99919	**18663**	0.02378	0.04782	0.35961
Average	0.04483	0.01852	1.37230				
1M Postflight							
11316	0.03792	0.00231	1.99524	**12854**	0.05749	0.00418	1.98423
11321	0.03989	0.00245	1.99472	**12857**	0.04818	0.00286	1.99832
11340	0.06009	0.00385	1.99753	**12883**	0.02833	0.00205	1.98845
11341	0.06125	0.00405	1.99493	**17222**	0.03596	0.00549	0.35801
11344	0.06899	0.00461	1.99641	**17223**	0.02191	0.00613	0.48741
11346	0.05040	0.00297	1.99909	**17226**	0.03516	0.00627	0.34973
11347	0.09554	0.00866	1.98644	**17239**	0.02765	0.00860	0.38200
11348	0.09725	0.00899	1.98595	**17241**	0.04749	0.00744	0.26812
12396	0.07767	0.00656	1.98702	**18657**	0.03448	0.01011	0.36721
12849	0.03680	0.00223	1.99611	**18660**	0.02754	0.00838	0.39019
12850	0.02863	0.00179	1.99408	**18662**	0.03280	0.01135	0.35460
12851	0.04715	0.00278	1.99943	**18663**	0.02629	0.01779	0.40104
Average	0.04687	0.00591	1.38568				
2M Postflight							
11316	0.03905	0.00236	1.99658	**12854**	0.05820	0.00719	1.99326
11321	0.04100	0.00250	1.99560	**12857**	0.04907	0.00288	2.00023
11340	0.06147	0.00397	1.99722	**12883**	0.02895	0.00683	2.00012
11341	0.06276	0.00418	1.99459	**17222**	0.03654	0.04261	0.38192
11344	0.07033	0.00475	1.99606	**17223**	0.02290	0.03941	0.51836
11346	0.05159	0.00305	1.99889	**17226**	0.03549	0.04614	0.37290
11347	0.09714	0.00897	1.98579	**17239**	0.02803	0.05132	0.40858
11348	0.09868	0.00927	1.98536	**17241**	0.04753	0.04534	0.28392
12396	0.07851	0.00666	1.99120	**18657**	0.03532	0.03690	0.38867
12849	0.03771	0.00258	1.99939	**18660**	0.02806	0.04589	0.41594
12850	0.02947	0.00267	2.00038	**18662**	0.03332	0.04453	0.37102
12851	0.04822	0.00284	1.99978	**18663**	0.02632	0.06228	0.41170
Average	0.04774	0.02021	1.39531				

Element	Damage (mm/mm^2 bone tissue)	BMU Activation Frequency ($BMUs/mm^2/day$)	Density (g/cm^3)	Element	Damage (mm/mm^2 bone tissue)	BMU Activation Frequency ($BMUs/mm^2/day$)	Density (g/cm^3)
3M Postflight							
11316	0.04012	0.00241	1.99701	**12854**	0.05887	0.00870	1.99236
11321	0.04206	0.00256	1.99585	**12857**	0.04993	0.00292	2.00089
11340	0.06274	0.00408	1.99688	**12883**	0.02952	0.00427	1.99863
11341	0.06417	0.00432	1.99420	**17222**	0.04026	0.01748	0.36443
11344	0.07156	0.00488	1.99566	**17223**	0.02505	0.02162	0.50572
11346	0.05271	0.00312	1.99867	**17226**	0.03952	0.01490	0.35454
11347	0.09854	0.00925	1.98492	**17239**	0.03118	0.02120	0.39068
11348	0.09988	0.00953	1.98455	**17241**	0.05377	0.01419	0.26508
12396	0.07926	0.00715	1.99260	**18657**	0.03928	0.01379	0.37444
12849	0.03853	0.00257	2.00029	**18660**	0.03104	0.01857	0.39801
12850	0.03021	0.00246	2.00151	**18662**	0.03754	0.01422	0.35731
12851	0.04923	0.00290	1.99981	**18663**	0.03034	0.01240	0.39221
Average	0.04981	0.00915	1.38901				
4M Postflight							
11316	0.04122	0.00248	1.99686	**12854**	0.05972	0.00675	1.98808
11321	0.04313	0.00262	1.99570	**12857**	0.05079	0.00297	2.00080
11340	0.06401	0.00420	1.99655	**12883**	0.03024	0.00426	1.99793
11341	0.06557	0.00446	1.99382	**17222**	0.04402	0.01504	0.36486
11344	0.07276	0.00501	1.99528	**17223**	0.02768	0.01774	0.50249
11346	0.05383	0.00320	1.99846	**17226**	0.04303	0.01540	0.35835
11347	0.09986	0.00953	1.98409	**17239**	0.03423	0.02103	0.39236
11348	0.10100	0.00977	1.98380	**17241**	0.05783	0.01463	0.27004
12396	0.07996	0.00719	1.99179	**18657**	0.04273	0.01270	0.37759
12849	0.03940	0.00257	1.99995	**18660**	0.03403	0.01896	0.39893
12850	0.03106	0.00244	2.00113	**18662**	0.04038	0.02350	0.36291
12851	0.05024	0.00296	1.99964	**18663**	0.03218	0.03468	0.40673
Average	0.05162	0.01017	1.38992				
5M Postflight							
11316	0.04230	0.00255	1.99668	**12854**	0.06040	0.00739	1.98927
11321	0.04417	0.00268	1.99553	**12857**	0.05162	0.00302	2.00066
11340	0.06523	0.00431	1.99621	**12883**	0.03085	0.00527	1.99912
11341	0.06692	0.00459	1.99343	**17222**	0.04620	0.02285	0.37138
11344	0.07389	0.00514	1.99491	**17223**	0.02956	0.02384	0.50742
11346	0.05491	0.00328	1.99824	**17226**	0.04509	0.02483	0.36428
11347	0.10103	0.00978	1.98330	**17239**	0.03601	0.03027	0.39754
11348	0.10198	0.00998	1.98311	**17241**	0.06002	0.02445	0.27610
12396	0.08058	0.00730	1.99131	**18657**	0.04527	0.01950	0.38309
12849	0.04023	0.00265	1.99984	**18660**	0.03588	0.02603	0.40362
12850	0.03183	0.00261	2.00116	**18662**	0.04281	0.02352	0.36300
12851	0.05121	0.00303	1.99946	**18663**	0.03386	0.03094	0.40311
Average	0.05299	0.01249	1.39132				
6M Postflight							
11316	0.04335	0.00261	1.99649	**12854**	0.06102	0.00790	1.98964
11321	0.04520	0.00275	1.99535	**12857**	0.05243	0.00308	2.00051
11340	0.06639	0.00443	1.99589	**12883**	0.03148	0.00452	1.99835
11341	0.06822	0.00472	1.99305	**17222**	0.04945	0.01718	0.36712
11344	0.07496	0.00526	1.99454	**17223**	0.03172	0.01991	0.50392
11346	0.05596	0.00335	1.99802	**17226**	0.04856	0.01618	0.35831
11347	0.10211	0.01000	1.98258	**17239**	0.03888	0.02019	0.39150
11348	0.10288	0.01017	1.98249	**17241**	0.06488	0.01573	0.26955
12396	0.08116	0.00744	1.99102	**18657**	0.04862	0.01458	0.37866
12849	0.04105	0.00268	1.99973	**18660**	0.03856	0.01906	0.39847
12850	0.03260	0.00256	2.00085	**18662**	0.04631	0.01660	0.35953
12851	0.05217	0.00309	1.99928	**18663**	0.03702	0.01884	0.39766
Average	0.05479	0.00970	1.38927				
7M Postflight							
11316	0.04439	0.00268	1.99630	**12854**	0.06166	0.00757	1.98860
11321	0.04621	0.00281	1.99517	**12857**	0.05322	0.00313	2.00035
11340	0.06752	0.00454	1.99557	**12883**	0.03210	0.00480	1.99845
11341	0.06947	0.00485	1.99267	**17222**	0.05279	0.01593	0.36643
11344	0.07599	0.00538	1.99419	**17223**	0.03403	0.01790	0.50246
11346	0.05699	0.00343	1.99781	**17226**	0.05180	0.01595	0.35897
11347	0.10310	0.01021	1.98192	**17239**	0.04153	0.02096	0.39263
11348	0.10370	0.01034	1.98192	**17241**	0.06908	0.01479	0.27013
12396	0.08168	0.00750	1.99070	**18657**	0.05214	0.01212	0.37860
12849	0.04185	0.00274	1.99959	**18660**	0.04119	0.01856	0.39829
12850	0.03336	0.00264	2.00066	**18662**	0.04904	0.02053	0.36156
12851	0.05310	0.00315	1.99910	**18663**	0.03886	0.02893	0.40297
Average	0.05645	0.01006	1.38938				

Element	Damage (mm/mm^2 bone tissue)	BMU Activation Frequency ($BMUs/mm^2/day$)	Density (g/cm^3)	Element	Damage (mm/mm^2 bone tissue)	BMU Activation Frequency ($BMUs/mm^2/day$)	Density (g/cm^3)
8M Postflight							
11316	0.04542	0.00274	1.99612	**12854**	0.06224	0.00779	1.98851
11321	0.04720	0.00287	1.99499	**12857**	0.05398	0.00319	2.00020
11340	0.06860	0.00465	1.99525	**12883**	0.03269	0.00491	1.99851
11341	0.07067	0.00498	1.99230	**17222**	0.05566	0.01720	0.36743
11344	0.07696	0.00549	1.99386	**17223**	0.03611	0.01887	0.50307
11346	0.05799	0.00350	1.99759	**17226**	0.05455	0.01788	0.36021
11347	0.10400	0.01040	1.98131	**17239**	0.04383	0.02249	0.39312
11348	0.10444	0.01050	1.98141	**17241**	0.07247	0.01729	0.27176
12396	0.08217	0.00758	1.99044	**18657**	0.05506	0.01510	0.38051
12849	0.04264	0.00277	1.99945	**18660**	0.04349	0.01968	0.39878
12850	0.03410	0.00267	2.00055	**18662**	0.05203	0.01769	0.36006
12851	0.05400	0.00322	1.99892	**18663**	0.04123	0.02239	0.39921
Average	0.05798	0.01024	1.38932				
9M Postflight							
11316	0.04642	0.00280	1.99594	**12854**	0.06279	0.00790	1.98837
11321	0.04817	0.00293	1.99482	**12857**	0.05473	0.00324	2.00005
11340	0.06964	0.00475	1.99495	**12883**	0.03328	0.00475	1.99825
11341	0.07183	0.00511	1.99194	**17222**	0.05885	0.01539	0.36605
11344	0.07789	0.00560	1.99353	**17223**	0.03828	0.01764	0.50165
11346	0.05896	0.00358	1.99738	**17226**	0.05780	0.01522	0.35821
11347	0.10484	0.01058	1.98076	**17239**	0.04657	0.01884	0.39070
11348	0.10512	0.01065	1.98095	**17241**	0.07683	0.01445	0.26956
12396	0.08261	0.00766	1.99021	**18657**	0.05838	0.01267	0.37875
12849	0.04341	0.00282	1.99934	**18660**	0.04608	0.01750	0.39682
12850	0.03483	0.00270	2.00043	**18662**	0.05518	0.01665	0.35930
12851	0.05488	0.00328	1.99874	**18663**	0.04382	0.02097	0.39824
Average	0.05963	0.00949	1.38854				
10M Postflight							
11316	0.04741	0.00286	1.99576	**12854**	0.06331	0.00791	1.98805
11321	0.04912	0.00299	1.99465	**12857**	0.05546	0.00329	1.99990
11340	0.07063	0.00485	1.99465	**12883**	0.03386	0.00487	1.99832
11341	0.07294	0.00523	1.99158	**17222**	0.06206	0.01474	0.36552
11344	0.07877	0.00571	1.99322	**17223**	0.04050	0.01656	0.50057
11346	0.05990	0.00365	1.99717	**17226**	0.06097	0.01477	0.35800
11347	0.10560	0.01074	1.98025	**17239**	0.04916	0.01890	0.39079
11348	0.10574	0.01078	1.98053	**17241**	0.08105	0.01372	0.26925
12396	0.08303	0.00771	1.99000	**18657**	0.06178	0.01182	0.37846
12849	0.04417	0.00286	1.99922	**18660**	0.04864	0.01688	0.39612
12850	0.03555	0.00275	2.00033	**18662**	0.05809	0.01703	0.35928
12851	0.05574	0.00334	1.99856	**18663**	0.04598	0.02273	0.39881
Average	0.06123	0.00945	1.38829				
11M Postflight							
11316	0.04837	0.00292	1.99559	**12854**	0.06381	0.00800	1.98787
11321	0.05005	0.00305	1.99447	**12857**	0.05616	0.00334	1.99975
11340	0.07159	0.00495	1.99436	**12883**	0.03442	0.00485	1.99828
11341	0.07400	0.00534	1.99124	**17222**	0.06515	0.01464	0.36531
11344	0.07960	0.00581	1.99292	**17223**	0.04265	0.01637	0.50012
11346	0.06082	0.00373	1.99696	**17226**	0.06399	0.01487	0.35795
11347	0.10630	0.01089	1.97977	**17239**	0.05166	0.01873	0.39035
11348	0.10630	0.01089	1.98015	**17241**	0.08497	0.01404	0.26937
12396	0.08342	0.00777	1.98983	**18657**	0.06492	0.01254	0.37879
12849	0.04490	0.00290	1.99973	**18660**	0.05111	0.01668	0.39562
12850	0.03626	0.00277	2.00022	**18662**	0.06119	0.01558	0.35829
12851	0.05658	0.00340	1.99839	**18663**	0.04846	0.01978	0.39685
Average	0.06278	0.00933	1.38801				
12M Postflight							
11316	0.04932	0.00299	1.99542	**12854**	0.06428	0.00804	1.98770
11321	0.05096	0.00311	1.99430	**12857**	0.05685	0.00339	1.99960
11340	0.07250	0.00505	1.99407	**12883**	0.03497	0.00482	1.99823
11341	0.07502	0.00546	1.99090	**17222**	0.06835	0.01381	0.36456
11344	0.08039	0.00590	1.99263	**17223**	0.04482	0.01574	0.49922
11346	0.06171	0.00380	1.99675	**17226**	0.06718	0.01384	0.35707
11347	0.10693	0.01103	1.97934	**17239**	0.05433	0.01723	0.38914
11348	0.10681	0.01100	1.97981	**17241**	0.08925	0.01289	0.26842
12396	0.08380	0.00781	1.98968	**18657**	0.06825	0.01139	0.37793
12849	0.04564	0.00294	1.99898	**18660**	0.05367	0.01580	0.39454
12850	0.03698	0.00280	2.00036	**18662**	0.06424	0.01534	0.35784
12851	0.05739	0.00347	1.99821	**18663**	0.05089	0.01979	0.39635
Average	0.06436	0.00906	1.38754				

Table 10. Element Values for Measured Variables in Trabecular Bone

Element	Damage (mm/mm² bone tissue)	BMU Activation Frequency (BMUs/mm²/day)	Density (g/cm³)	Element	Damage (mm/mm² bone tissue)	BMU Activation Frequency (BMUs/mm²/day)	Density (g/cm³)
Earth Baseline Simulation							
8026	0.03061	0.01500	0.24055	**12339**	0.02207	0.10895	0.41446
8320	0.01430	0.05964	0.47873	**12347**	0.02214	0.07457	0.41399
8321	0.01364	0.06474	0.51258	**12764**	0.03218	0.17043	0.24996
8323	0.01375	0.06467	0.49282	**13072**	0.04004	0.17555	0.21584
8324	0.01455	0.05463	0.46746	**13092**	0.04082	0.00026	0.21392
8325	0.00845	0.06863	0.85265	**13097**	0.03163	0.00121	0.24899
8326	0.01037	0.07465	0.64351	**13211**	0.04022	0.17260	0.21251
8327	0.01117	0.06500	0.60796	**13229**	0.03659	0.13418	0.21512
9331	0.02204	0.09512	0.29740	**13383**	0.03546	0.00265	0.21432
9562	0.02404	0.00972	0.37697	**13391**	0.02787	0.00876	0.28451
9606	0.02527	0.01001	0.27649	**13393**	0.03169	0.00059	0.24293
9608	0.01704	0.05671	0.39304	**13736**	0.03691	0.16056	0.22624
9709	0.01496	0.04619	0.47840	**14143**	0.02289	0.06640	0.39452
9711	0.01357	0.03334	0.50595	**14150**	0.02510	0.06513	0.34948
9712	0.01392	0.04240	0.49604	**14624**	0.03876	0.02734	0.20101
9713	0.01603	0.03346	0.40860	**14639**	0.03538	0.05502	0.21915
9716	0.02804	0.02657	0.23843	**14778**	0.04077	0.13951	0.21013
9741	0.01039	0.05272	0.67828	**14786**	0.04396	0.12052	0.18787
9743	0.01093	0.06909	0.63309	**14920**	0.03362	0.16759	0.23819
9765	0.00776	0.06258	1.13970	**14955**	0.04683	0.08767	0.19790
9766	0.00806	0.05902	1.14261	**15287**	0.04129	0.00276	0.19820
9767	0.00835	0.07140	0.92867	**15301**	0.04658	0.06897	0.19606
9779	0.01371	0.08026	0.47845	**15761**	0.03545	0.07311	0.23704
9781	0.01056	0.06438	0.62828	**16117**	0.04955	0.03150	0.18646
9782	0.00904	0.07362	0.75383	**16258**	0.05897	0.00311	0.15015
9783	0.00966	0.08360	0.68071	**16706**	0.04050	0.19015	0.20659
9785	0.01006	0.08670	0.65456	**16726**	0.04209	0.15549	0.20142
9805	0.00790	0.06650	1.13897	**16729**	0.04574	0.12987	0.18840
9808	0.00893	0.08583	0.76426	**24095**	0.02360	0.05013	0.33128
9810	0.00919	0.09141	0.70539	**24242**	0.02913	0.19416	0.24842
9811	0.00818	0.05537	1.31324	**24386**	0.02269	0.22163	0.32161
9812	0.01030	0.07593	0.71189	**24510**	0.02224	0.09860	0.30485
9823	0.00932	0.10107	0.70845	**24612**	0.01424	0.13572	0.48166
9825	0.00747	0.08348	1.02409	**24619**	0.01525	0.15366	0.45076
9828	0.00792	0.09974	0.83946	**24665**	0.01616	0.13776	0.41723
9829	0.00877	0.07021	1.10772	**24703**	0.01751	0.07375	0.37155
10052	0.02207	0.06657	0.41243	**24741**	0.01105	0.11574	0.57986
10055	0.01083	0.05385	0.65426	**24787**	0.01303	0.10235	0.50149
10067	0.03626	0.00023	0.21593	**24788**	0.01391	0.07459	0.49256
10116	0.01021	0.04439	1.39881	**24789**	0.01528	0.04135	0.44824
10117	0.00953	0.05304	1.31623	**24806**	0.01089	0.10800	0.58599
10118	0.00971	0.07981	0.73627	**24830**	0.01354	0.04302	0.46986
10123	0.00799	0.06326	1.24210	**24862**	0.01226	0.04841	0.51043
10124	0.00790	0.08082	1.06747	**24863**	0.01338	0.03810	0.46777
11182	0.02153	0.08669	0.43257	**24864**	0.01152	0.06527	0.54526
11241	0.02272	0.10025	0.39721	**24865**	0.01017	0.08434	0.61244
11313	0.01045	0.12311	0.60218	**24866**	0.00845	0.08900	0.75912
11600	0.02995	0.10440	0.26981	**24867**	0.00758	0.08869	0.90303
11738	0.03953	0.00714	0.21525	**24874**	0.01926	0.00513	0.35057
11791	0.04500	0.00023	0.18921	**24875**	0.01652	0.01628	0.40061
11881	0.02698	0.00250	0.27624	**24906**	0.00956	0.07613	0.65574
Average	0.02129	0.07427	0.50148				
Space Simulation							
8026	0.04060	0.05186	0.23073	**12339**	0.03101	0.02628	0.36869
8320	0.01862	0.03811	0.38341	**12347**	0.03098	0.03417	0.37417
8321	0.01778	0.04441	0.41710	**12764**	0.05220	0.00382	0.19866
8323	0.01832	0.04389	0.39987	**13072**	0.06862	0.00051	0.16042
8324	0.01898	0.06018	0.37506	**13092**	0.05629	0.00076	0.17585
8325	0.00795	0.09918	0.65852	**13097**	0.04259	0.00895	0.20556
8326	0.01205	0.07069	0.50025	**13211**	0.06732	0.03321	0.16120
8327	0.01328	0.06857	0.47408	**13229**	0.06078	0.07932	0.17968
9331	0.03695	0.02076	0.22082	**13383**	0.04632	0.12532	0.20209
9562	0.03220	0.03301	0.35516	**13391**	0.03857	0.00368	0.23506
9606	0.03504	0.08516	0.23073	**13393**	0.03889	0.04730	0.21967
9608	0.02441	0.02487	0.30565	**13736**	0.06408	0.02751	0.17145
9709	0.01997	0.06772	0.37375	**14143**	0.03260	0.03438	0.36096
9711	0.01623	0.06377	0.38015	**14150**	0.03615	0.03025	0.32175

Element	Damage (mm/mm² bone tissue)	BMU Activation Frequency (BMUs/mm²/day)	Density (g/cm³)	Element	Damage (mm/mm² bone tissue)	BMU Activation Frequency (BMUs/mm²/day)	Density (g/cm³)
9712	0.01738	0.07482	0.38353	**14624**	0.05492	0.07521	0.19365
9713	0.02160	0.07433	0.30132	**14639**	0.05495	0.16478	0.19229
9716	0.04043	0.12497	0.20605	**14778**	0.06979	0.01840	0.15300
9741	0.01133	0.07345	0.52279	**14786**	0.07281	0.05991	0.15914
9743	0.01299	0.06764	0.49566	**14920**	0.05654	0.02802	0.19307
9765	0.00561	0.12055	0.91284	**14955**	0.07989	0.00042	0.14099
9766	0.00591	0.11296	0.92890	**15287**	0.05671	0.00363	0.16020
9767	0.00740	0.10166	0.73459	**15301**	0.07651	0.00024	0.14473
9779	0.01870	0.05324	0.38645	**15761**	0.05443	0.02723	0.20734
9781	0.01258	0.08091	0.49986	**16117**	0.07555	0.01633	0.16248
9782	0.00948	0.09262	0.58248	**16258**	0.08042	0.06446	0.14581
9783	0.01101	0.09557	0.52989	**16706**	0.07143	0.00351	0.15979
9785	0.01187	0.08787	0.51516	**16726**	0.06974	0.04093	0.16774
9805	0.00606	0.10821	0.93878	**16729**	0.07477	0.05092	0.15881
9808	0.00918	0.10207	0.59005	**24095**	0.03539	0.04342	0.31348
9810	0.01017	0.09889	0.54209	**24242**	0.05129	0.06002	0.20318
9811	0.00568	0.10357	1.11878	**24386**	0.03843	0.01018	0.23233
9812	0.01152	0.07496	0.58508	**24510**	0.03628	0.12866	0.24996
9823	0.01061	0.07060	0.55314	**24612**	0.02024	0.04192	0.38278
9825	0.00631	0.10737	0.81522	**24619**	0.02255	0.03201	0.35972
9828	0.00776	0.09947	0.63705	**24665**	0.02464	0.05039	0.34243
9829	0.00680	0.11114	0.90349	**24703**	0.02631	0.12386	0.32105
10052	0.03016	0.02191	0.36505	**24741**	0.01456	0.06755	0.46288
10055	0.01164	0.09472	0.50102	**24787**	0.01843	0.07129	0.41670
10067	0.04572	0.05314	0.21853	**24788**	0.01907	0.08047	0.41687
10116	0.00730	0.08695	1.23259	**24789**	0.02066	0.08319	0.39079
10117	0.00685	0.09510	1.13440	**24806**	0.01431	0.07808	0.47435
10118	0.01059	0.08201	0.59772	**24830**	0.01797	0.10363	0.40539
10123	0.00588	0.09957	1.04589	**24862**	0.01558	0.11319	0.42518
10124	0.00636	0.10080	0.85891	**24863**	0.01723	0.12734	0.39980
11182	0.02934	0.01907	0.38314	**24864**	0.01478	0.10686	0.45109
11241	0.03177	0.01525	0.34962	**24865**	0.01267	0.09618	0.48923
11313	0.01336	0.06227	0.46499	**24866**	0.00922	0.11081	0.60014
11600	0.04471	0.00709	0.22667	**24867**	0.00727	0.11117	0.71387
11738	0.05569	0.00468	0.18154	**24874**	0.02504	0.02193	0.31168
11791	0.06187	0.00314	0.16165	**24875**	0.02161	0.07317	0.35735
11881	0.03574	0.01254	0.24580	**24906**	0.01121	0.11241	0.52549
Average	0.03019	0.06298	0.41055				
1M Postflight							
8026	0.05003	0.00445	0.24434	**12339**	0.03362	0.01867	0.39846
8320	0.02256	0.00308	0.42405	**12347**	0.03404	0.01396	0.40037
8321	0.02094	0.00552	0.46080	**12764**	0.05067	0.03586	0.24277
8323	0.02159	0.00532	0.44315	**13072**	0.06221	0.04365	0.20609
8324	0.02311	0.00411	0.40900	**13092**	0.05870	0.00769	0.21874
8325	0.01023	0.00788	0.71876	**13097**	0.04862	0.00479	0.24130
8326	0.01479	0.00740	0.55293	**13211**	0.06318	0.03255	0.19465
8327	0.01619	0.00632	0.52336	**13229**	0.06053	0.01726	0.20166
9331	0.03541	0.02808	0.27265	**13383**	0.05347	0.00225	0.21663
9562	0.03801	0.00064	0.37006	**13391**	0.04096	0.01104	0.28276
9606	0.04545	0.00035	0.24167	**13393**	0.04754	0.00098	0.23995
9608	0.02599	0.01857	0.35938	**13736**	0.06027	0.02565	0.20464
9709	0.02332	0.00421	0.41388	**14143**	0.03564	0.01524	0.38649
9711	0.02043	0.00220	0.41950	**14150**	0.03945	0.01512	0.34742
9712	0.02129	0.00319	0.42067	**14624**	0.06330	0.00591	0.20283
9713	0.02618	0.00236	0.33768	**14639**	0.06125	0.00450	0.20041
9716	0.04977	0.00286	0.21594	**14778**	0.06573	0.03106	0.19230
9741	0.01400	0.00711	0.57758	**14786**	0.07192	0.02398	0.17985
9743	0.01555	0.00831	0.54891	**14920**	0.05417	0.02700	0.22298
9765	0.00739	0.00814	0.97562	**14955**	0.07251	0.03278	0.18757
9766	0.00768	0.00764	0.98931	**15287**	0.06008	0.00859	0.19991
9767	0.00944	0.00917	0.79517	**15301**	0.06943	0.03975	0.18988
9779	0.02185	0.00875	0.42832	**15761**	0.05722	0.01841	0.23252
9781	0.01547	0.00645	0.54607	**16117**	0.07890	0.00929	0.18410
9782	0.01191	0.00824	0.63948	**16258**	0.09138	0.00108	0.15640
9783	0.01358	0.00852	0.58048	**16706**	0.06507	0.04417	0.19682
9785	0.01445	0.00869	0.56466	**16726**	0.06685	0.02743	0.19374
9805	0.00780	0.00864	0.99828	**16729**	0.07241	0.02087	0.18220
9808	0.01155	0.00900	0.64532	**24095**	0.03727	0.01894	0.34263
9810	0.01264	0.00922	0.59650	**24242**	0.04894	0.01323	0.22553
9811	0.00723	0.00751	1.17445	**24386**	0.03576	0.03562	0.28252

Element	Damage (mm/mm² bone tissue)	BMU Activation Frequency (BMUs/mm²/day)	Density (g/cm³)	Element	Damage (mm/mm² bone tissue)	BMU Activation Frequency (BMUs/mm²/day)	Density (g/cm³)
9812	0.01403	0.00776	0.63076	**24510**	0.03750	0.01217	0.27569
9823	0.01291	0.01161	0.61148	**24612**	0.02220	0.01697	0.43222
9825	0.00816	0.01065	0.88079	**24619**	0.02415	0.01959	0.40980
9828	0.00986	0.01234	0.70311	**24665**	0.02630	0.01887	0.38461
9829	0.00856	0.00804	0.96138	**24703**	0.02965	0.00954	0.34412
10052	0.03351	0.01025	0.39457	**24741**	0.01682	0.01489	0.51241
10055	0.01472	0.00455	0.54497	**24787**	0.02084	0.01413	0.45583
10067	0.05718	0.00040	0.22694	**24788**	0.02213	0.00816	0.44911
10116	0.00874	0.00612	1.28012	**24789**	0.02500	0.00309	0.41295
10117	0.00836	0.00697	1.18641	**24806**	0.01667	0.01348	0.52025
10118	0.01303	0.00824	0.64594	**24830**	0.02233	0.00330	0.42627
10123	0.00747	0.00828	1.10531	**24862**	0.01967	0.00316	0.44998
10124	0.00813	0.01046	0.92355	**24863**	0.02219	0.00169	0.41504
11182	0.03221	0.01482	0.41446	**24864**	0.01805	0.00629	0.48389
11241	0.03430	0.01936	0.38333	**24865**	0.01528	0.01022	0.53464
11313	0.01554	0.01607	0.52199	**24866**	0.01151	0.01042	0.65371
11600	0.04517	0.02858	0.26740	**24867**	0.00929	0.01091	0.77565
11738	0.06151	0.00374	0.21280	**24874**	0.03051	0.00284	0.34207
11791	0.06793	0.00235	0.19528	**24875**	0.02731	0.00117	0.37400
11881	0.04140	0.00479	0.27953	**24906**	0.01399	0.00732	0.56834
Average	0.03266	0.01189	0.44934				
2M Postflight							
8026	0.04815	0.04939	0.27806	**12339**	0.03445	0.03677	0.40296
8320	0.02300	0.04916	0.47207	**12347**	0.03492	0.03663	0.40572
8321	0.02157	0.04958	0.50216	**12764**	0.05176	0.03223	0.24293
8323	0.02219	0.04900	0.48511	**13072**	0.06424	0.02220	0.20626
8324	0.02359	0.03966	0.45973	**13092**	0.05580	0.04909	0.24102
8325	0.01093	0.05522	0.78710	**13097**	0.04647	0.05060	0.27208
8326	0.01540	0.05587	0.60672	**13211**	0.06555	0.01686	0.19742
8327	0.01684	0.04818	0.57741	**13229**	0.06229	0.01958	0.20777
9331	0.03592	0.03836	0.29281	**13383**	0.05151	0.03456	0.24276
9562	0.03871	0.04499	0.39576	**13391**	0.04025	0.05341	0.30651
9606	0.04276	0.04123	0.28947	**13393**	0.04505	0.04946	0.27807
9608	0.02631	0.04689	0.38940	**13736**	0.06131	0.02996	0.21425
9709	0.02378	0.04174	0.46062	**14143**	0.03662	0.03551	0.38872
9711	0.02082	0.04483	0.47866	**14150**	0.04046	0.03541	0.34983
9712	0.02185	0.04150	0.47420	**14624**	0.06250	0.03732	0.21712
9713	0.02602	0.04583	0.39199	**14639**	0.05905	0.03058	0.22408
9716	0.04661	0.02966	0.25581	**14778**	0.06711	0.01798	0.19410
9741	0.01467	0.04975	0.63597	**14786**	0.07497	0.02096	0.18246
9743	0.01624	0.04827	0.59900	**14920**	0.05615	0.02646	0.23084
9765	0.00812	0.04909	1.05230	**14955**	0.07273	0.02242	0.19183
9766	0.00845	0.04477	1.06173	**15287**	0.05767	0.03491	0.21522
9767	0.01015	0.05369	0.86054	**15301**	0.07129	0.01672	0.19083
9779	0.02242	0.04636	0.46966	**15761**	0.05857	0.03186	0.23294
9781	0.01615	0.05217	0.59856	**16117**	0.07916	0.03147	0.19141
9782	0.01258	0.05496	0.70029	**16258**	0.08712	0.04072	0.17297
9783	0.01421	0.05587	0.63589	**16706**	0.06927	0.01572	0.19690
9785	0.01510	0.05473	0.61556	**16726**	0.06948	0.02262	0.19905
9805	0.00846	0.05339	1.06739	**16729**	0.07441	0.02586	0.18766
9808	0.01222	0.05722	0.70669	**24095**	0.03805	0.04771	0.34975
9810	0.01327	0.05806	0.65398	**24242**	0.05002	0.02645	0.24842
9811	0.00790	0.04505	1.24251	**24386**	0.03700	0.03504	0.30187
9812	0.01479	0.05165	0.67867	**24510**	0.03729	0.03904	0.30217
9823	0.01352	0.06042	0.66394	**24612**	0.02285	0.04585	0.46161
9825	0.00880	0.05949	0.95090	**24619**	0.02486	0.04474	0.43407
9828	0.01046	0.06396	0.76893	**24665**	0.02702	0.04265	0.40596
9829	0.00925	0.04983	1.03289	**24703**	0.03002	0.04359	0.37344
10052	0.03389	0.04809	0.40791	**24741**	0.01742	0.05559	0.55015
10055	0.01561	0.03980	0.60644	**24787**	0.02151	0.04943	0.48558
10067	0.05510	0.04432	0.26049	**24788**	0.02274	0.05125	0.48188
10116	0.00941	0.03622	1.33900	**24789**	0.02553	0.05143	0.45127
10117	0.00905	0.03989	1.25038	**24806**	0.01727	0.05674	0.55828
10118	0.01377	0.05382	0.69703	**24830**	0.02287	0.05276	0.47011
10123	0.00815	0.04782	1.17337	**24862**	0.02017	0.05819	0.49973
10124	0.00880	0.05464	0.99281	**24863**	0.02257	0.05523	0.46620
11182	0.03279	0.04169	0.42337	**24864**	0.01858	0.05941	0.52820
11241	0.03493	0.04030	0.38915	**24865**	0.01585	0.06081	0.58090
11313	0.01608	0.05918	0.56402	**24866**	0.01208	0.06490	0.71070
11600	0.04576	0.03888	0.27072	**24867**	0.00988	0.06437	0.84067

Element	Damage (mm/mm^2 bone tissue)	BMU Activation Frequency ($BMUs/mm^2/day$)	Density (g/cm^3)	Element	Damage (mm/mm^2 bone tissue)	BMU Activation Frequency ($BMUs/mm^2/day$)	Density (g/cm^3)
11738	0.05918	0.03885	0.23457	**24874**	0.03036	0.05994	0.38170
11791	0.06381	0.04329	0.22092	**24875**	0.02763	0.05166	0.41828
11881	0.04103	0.04726	0.31024	**24906**	0.01455	0.06397	0.62208
Average	0.03299	0.04424	0.48470				
3M Postflight							
8026	0.05219	0.01143	0.26408	**12339**	0.03819	0.01642	0.39105
8320	0.02486	0.02405	0.45496	**12347**	0.03867	0.01540	0.39415
8321	0.02354	0.02708	0.48270	**12764**	0.05796	0.01651	0.23570
8323	0.02423	0.02634	0.46652	**13072**	0.07036	0.01590	0.20512
8324	0.02530	0.02890	0.44967	**13092**	0.06253	0.00573	0.22905
8325	0.01180	0.04212	0.77447	**13097**	0.05099	0.00865	0.25988
8326	0.01673	0.03550	0.58826	**13211**	0.07127	0.01526	0.20148
8327	0.01827	0.03379	0.56360	**13229**	0.06956	0.01173	0.20801
9331	0.04083	0.01755	0.28451	**13383**	0.05595	0.01881	0.24228
9562	0.04144	0.01350	0.37870	**13391**	0.04526	0.00900	0.28944
9606	0.04542	0.01701	0.28472	**13393**	0.04833	0.01698	0.26950
9608	0.02969	0.01927	0.37581	**13736**	0.06757	0.01235	0.21191
9709	0.02596	0.02870	0.44797	**14143**	0.04069	0.01470	0.37760
9711	0.02221	0.03194	0.46936	**14150**	0.04501	0.01367	0.33951
9712	0.02342	0.03259	0.46397	**14624**	0.06917	0.01611	0.21099
9713	0.02802	0.03285	0.37904	**14639**	0.06472	0.01592	0.22352
9716	0.04978	0.02032	0.26020	**14778**	0.07309	0.01605	0.19711
9741	0.01597	0.03449	0.62403	**14786**	0.08254	0.01615	0.18129
9743	0.01777	0.03343	0.58442	**14920**	0.06176	0.01431	0.22946
9765	0.00877	0.04263	1.04754	**14955**	0.07907	0.01555	0.19015
9766	0.00913	0.04029	1.05781	**15287**	0.06330	0.01330	0.21413
9767	0.01098	0.04191	0.84840	**15301**	0.07650	0.01656	0.19378
9779	0.02456	0.02688	0.45390	**15761**	0.06565	0.01299	0.22595
9781	0.01745	0.03659	0.58144	**16117**	0.08872	0.00953	0.18325
9782	0.01368	0.03870	0.68656	**16258**	0.09708	0.01320	0.16469
9783	0.01541	0.04228	0.61828	**16706**	0.07446	0.01988	0.19818
9785	0.01643	0.03941	0.59732	**16726**	0.07619	0.01791	0.19676
9805	0.00908	0.04121	1.05663	**16729**	0.08314	0.01584	0.18246
9808	0.01320	0.04576	0.68998	**24095**	0.04300	0.01407	0.33180
9810	0.01439	0.04501	0.63535	**24242**	0.05407	0.01850	0.25034
9811	0.00849	0.03637	1.23724	**24386**	0.04107	0.01880	0.29510
9812	0.01596	0.03730	0.66094	**24510**	0.04202	0.02242	0.29494
9823	0.01473	0.04067	0.64212	**24612**	0.02555	0.02528	0.44447
9825	0.00950	0.04556	0.93617	**24619**	0.02797	0.02264	0.41705
9828	0.01134	0.04885	0.74975	**24665**	0.03052	0.02271	0.39096
9829	0.00992	0.04342	1.02438	**24703**	0.03343	0.02557	0.36119
10052	0.03752	0.01461	0.39050	**24741**	0.01927	0.03631	0.52905
10055	0.01678	0.03749	0.60102	**24787**	0.02388	0.03179	0.46724
10067	0.05868	0.01356	0.24987	**24788**	0.02494	0.03120	0.46201
10116	0.01003	0.02829	1.33593	**24789**	0.02747	0.02917	0.43158
10117	0.00967	0.03321	1.24626	**24806**	0.01904	0.03813	0.53659
10118	0.01486	0.03990	0.67915	**24830**	0.02444	0.03570	0.45124
10123	0.00878	0.03669	1.16542	**24862**	0.02143	0.04217	0.47793
10124	0.00951	0.04250	0.98088	**24863**	0.02378	0.03967	0.44696
11182	0.03627	0.01556	0.40894	**24864**	0.02010	0.04113	0.50583
11241	0.03877	0.01647	0.37563	**24865**	0.01727	0.04363	0.55826
11313	0.01780	0.03801	0.54165	**24866**	0.01307	0.04791	0.68865
11600	0.05158	0.01601	0.26078	**24867**	0.01068	0.04833	0.82131
11738	0.06496	0.00913	0.22823	**24874**	0.03285	0.01704	0.35941
11791	0.07013	0.00604	0.21322	**24875**	0.02924	0.02745	0.39934
11881	0.04487	0.01022	0.29435	**24906**	0.01564	0.04725	0.59863
Average	0.03617	0.02640	0.47313				
4M Postflight							
8026	0.05727	0.01043	0.26986	**12339**	0.04044	0.02310	0.39579
8320	0.02819	0.01451	0.45220	**12347**	0.04105	0.02170	0.39872
8321	0.02645	0.01742	0.47879	**12764**	0.06016	0.02949	0.24202
8323	0.02727	0.01704	0.46294	**13072**	0.07291	0.02898	0.20924
8324	0.02881	0.01293	0.44290	**13092**	0.06570	0.02336	0.24011
8325	0.01343	0.02754	0.76225	**13097**	0.05525	0.01912	0.26786
8326	0.01896	0.02409	0.58050	**13211**	0.07449	0.02362	0.20379
8327	0.02073	0.02034	0.55527	**13229**	0.07310	0.01888	0.21238
9331	0.04405	0.01973	0.29037	**13383**	0.06100	0.01466	0.24288
9562	0.04534	0.01167	0.38069	**13391**	0.04850	0.02377	0.29871
9606	0.05121	0.00678	0.28545	**13393**	0.05336	0.01615	0.27149
9608	0.03260	0.02258	0.37912	**13736**	0.07052	0.02550	0.21631

Element	Damage (mm/mm² bone tissue)	BMU Activation Frequency (BMUs/mm²/day)	Density (g/cm³)	Element	Damage (mm/mm² bone tissue)	BMU Activation Frequency (BMUs/mm²/day)	Density (g/cm³)
9709	0.02938	0.01581	0.44120	**14143**	0.04299	0.02268	0.38298
9711	0.02548	0.01798	0.46043	**14150**	0.04746	0.02372	0.34543
9712	0.02676	0.01644	0.45426	**14624**	0.07379	0.01922	0.21293
9713	0.03219	0.01635	0.37011	**14639**	0.06972	0.01362	0.22457
9716	0.05523	0.00906	0.26020	**14778**	0.07613	0.02523	0.19961
9741	0.01811	0.02383	0.61517	**14786**	0.08703	0.01951	0.18239
9743	0.02002	0.02232	0.57655	**14920**	0.06492	0.02278	0.23320
9765	0.00993	0.02895	1.03321	**14955**	0.08195	0.02944	0.19410
9766	0.01030	0.02704	1.04390	**15287**	0.06652	0.02933	0.21975
9767	0.01240	0.02909	0.83599	**15301**	0.07961	0.03119	0.19598
9779	0.02761	0.01704	0.45041	**15761**	0.06830	0.02535	0.23256
9781	0.01979	0.02172	0.57245	**16117**	0.09281	0.01916	0.18860
9782	0.01554	0.02607	0.67679	**16258**	0.10256	0.01723	0.16774
9783	0.01744	0.02651	0.60664	**16706**	0.07883	0.02200	0.19843
9785	0.01854	0.02517	0.58746	**16726**	0.08052	0.02018	0.19687
9805	0.01021	0.02845	1.04465	**16729**	0.08756	0.01949	0.18348
9808	0.01496	0.02924	0.67618	**24095**	0.04540	0.02176	0.33961
9810	0.01632	0.02815	0.62269	**24242**	0.05769	0.01820	0.25071
9811	0.00946	0.02618	1.22589	**24386**	0.04405	0.02347	0.29885
9812	0.01788	0.02451	0.65097	**24510**	0.04544	0.01641	0.29496
9823	0.01657	0.02965	0.63242	**24612**	0.02817	0.02082	0.44372
9825	0.01071	0.03317	0.92271	**24619**	0.03062	0.02118	0.41823
9828	0.01283	0.03583	0.73525	**24665**	0.03326	0.01975	0.39219
9829	0.01111	0.02862	1.00963	**24703**	0.03683	0.01526	0.35990
10052	0.04004	0.02163	0.39632	**24741**	0.02139	0.02732	0.52212
10055	0.01916	0.02061	0.58770	**24787**	0.02632	0.02259	0.46234
10067	0.06485	0.01021	0.25131	**24788**	0.02768	0.01960	0.45723
10116	0.01102	0.02000	1.32769	**24789**	0.03085	0.01571	0.42699
10117	0.01070	0.02304	1.23568	**24806**	0.02114	0.02702	0.52864
10118	0.01668	0.02657	0.66799	**24830**	0.02771	0.01748	0.44305
10123	0.00982	0.02681	1.15464	**24862**	0.02448	0.02028	0.46686
10124	0.01069	0.03145	0.96806	**24863**	0.02727	0.01685	0.43687
11182	0.03856	0.02283	0.41422	**24864**	0.02266	0.02328	0.49613
11241	0.04101	0.02494	0.38092	**24865**	0.01940	0.02826	0.54730
11313	0.01985	0.03026	0.53425	**24866**	0.01473	0.03189	0.67573
11600	0.05381	0.02872	0.26725	**24867**	0.01202	0.03450	0.80744
11738	0.06918	0.02084	0.23402	**24874**	0.03673	0.01739	0.36201
11791	0.07454	0.01698	0.22172	**24875**	0.03326	0.01420	0.39471
11881	0.04948	0.01426	0.29959	**24906**	0.01771	0.02795	0.58579
Average	0.03906	0.02217	0.47016				
5M Postflight							
8026	0.05847	0.03357	0.27889	**12339**	0.04263	0.02068	0.39655
8320	0.02983	0.02880	0.46428	**12347**	0.04322	0.02047	0.39954
8321	0.02810	0.02809	0.48953	**12764**	0.06430	0.01839	0.23942
8323	0.02898	0.02775	0.47358	**13072**	0.07905	0.01428	0.20467
8324	0.03073	0.02503	0.45531	**13092**	0.06874	0.01990	0.23837
8325	0.01453	0.03720	0.77156	**13097**	0.05721	0.02729	0.26998
8326	0.02030	0.03463	0.59052	**13211**	0.08144	0.01302	0.19994
8327	0.02228	0.02986	0.56555	**13229**	0.07923	0.01413	0.21007
9331	0.04748	0.01979	0.29331	**13383**	0.06414	0.02470	0.24524
9562	0.04684	0.02583	0.38891	**13391**	0.05080	0.02354	0.29956
9606	0.05310	0.02894	0.29683	**13393**	0.05502	0.03022	0.27585
9608	0.03494	0.02431	0.38278	**13736**	0.07645	0.01621	0.21276
9709	0.03143	0.02457	0.45096	**14143**	0.04528	0.02001	0.38286
9711	0.02713	0.03139	0.47073	**14150**	0.05000	0.01981	0.34424
9712	0.02857	0.02809	0.46511	**14624**	0.07763	0.02045	0.21343
9713	0.03401	0.03055	0.38183	**14639**	0.07384	0.02148	0.22626
9716	0.05828	0.02364	0.26703	**14778**	0.08263	0.01356	0.19634
9741	0.01956	0.03083	0.62343	**14786**	0.09376	0.01426	0.18119
9743	0.02159	0.02878	0.58532	**14920**	0.07027	0.01668	0.23046
9765	0.01082	0.03565	1.03994	**14955**	0.08831	0.01278	0.18970
9766	0.01123	0.03286	1.05018	**15287**	0.07117	0.01742	0.21473
9767	0.01343	0.03641	0.84371	**15301**	0.08701	0.01186	0.18929
9779	0.02946	0.02669	0.46069	**15761**	0.07253	0.01858	0.22953
9781	0.02118	0.03313	0.58356	**16117**	0.09798	0.01591	0.18714
9782	0.01680	0.03495	0.68603	**16258**	0.10682	0.02119	0.16744
9783	0.01872	0.03650	0.61659	**16706**	0.08522	0.01348	0.19636
9785	0.01989	0.03475	0.59730	**16726**	0.08655	0.01588	0.19605
9805	0.01104	0.03764	1.05237	**16729**	0.09377	0.01661	0.18294
9808	0.01611	0.03908	0.68557	**24095**	0.04772	0.02381	0.34228

Element	Damage (mm/mm² bone tissue)	BMU Activation Frequency (BMUs/mm²/day)	Density (g/cm³)	Element	Damage (mm/mm² bone tissue)	BMU Activation Frequency (BMUs/mm²/day)	Density (g/cm³)
9810	0.01753	0.03884	0.63284	**24242**	0.06268	0.01700	0.25108
9811	0.01024	0.03289	1.23151	**24386**	0.04768	0.01963	0.29976
9812	0.01916	0.03234	0.66009	**24510**	0.04866	0.02311	0.29980
9823	0.01777	0.03747	0.64141	**24612**	0.03021	0.02431	0.45080
9825	0.01157	0.04206	0.92988	**24619**	0.03282	0.02305	0.42406
9828	0.01382	0.04394	0.74280	**24665**	0.03563	0.02278	0.39784
9829	0.01200	0.03677	1.01673	**24703**	0.03913	0.02537	0.36806
10052	0.04184	0.02371	0.39923	**24741**	0.02292	0.03243	0.53001
10055	0.02077	0.02826	0.59646	**24787**	0.02814	0.02805	0.47016
10067	0.06616	0.02851	0.25886	**24788**	0.02929	0.03023	0.46699
10116	0.01183	0.02633	1.33289	**24789**	0.03225	0.03288	0.43903
10117	0.01153	0.02946	1.24117	**24806**	0.02261	0.03361	0.53725
10118	0.01788	0.03461	0.67690	**24830**	0.02902	0.03592	0.45598
10123	0.01062	0.03452	1.16066	**24862**	0.02559	0.04149	0.48088
10124	0.01157	0.03869	0.97444	**24863**	0.02835	0.04099	0.45183
11182	0.04050	0.02183	0.41579	**24864**	0.02392	0.03859	0.50798
11241	0.04315	0.02152	0.38157	**24865**	0.02067	0.03896	0.55726
11313	0.02129	0.03487	0.54181	**24866**	0.01576	0.04375	0.68533
11600	0.05725	0.01957	0.26605	**24867**	0.01293	0.04474	0.81537
11738	0.07275	0.01840	0.23222	**24874**	0.03791	0.03413	0.37221
11791	0.07761	0.01977	0.22165	**24875**	0.03441	0.03631	0.40809
11881	0.05118	0.02898	0.30629	**24906**	0.01878	0.04370	0.59742
Average	0.04152	0.02755	0.47551				
6M Postflight							
8026	0.06407	0.01114	0.26879	**12339**	0.05577	0.01834	0.39481
8320	0.03209	0.02090	0.45900	**12347**	0.04545	0.01684	0.39750
8321	0.03011	0.02368	0.48551	**12764**	0.04616	0.02173	0.23986
8323	0.03111	0.02292	0.46956	**13072**	0.06839	0.02060	0.20716
8324	0.03294	0.02183	0.45226	**13092**	0.08323	0.01277	0.23536
8325	0.01560	0.03390	0.76840	**13097**	0.07487	0.01330	0.26383
8326	0.02179	0.02989	0.58642	**13211**	0.06270	0.01754	0.20250
8327	0.02393	0.02708	0.56283	**13229**	0.08614	0.01269	0.20998
9331	0.05144	0.02029	0.29127	**13383**	0.08527	0.01210	0.24052
9562	0.05008	0.01348	0.38290	**13391**	0.07012	0.01586	0.29574
9606	0.05792	0.01261	0.28783	**13393**	0.05522	0.01334	0.26981
9608	0.03789	0.02115	0.38023	**13736**	0.06021	0.01586	0.21305
9709	0.03375	0.02258	0.44855	**14143**	0.08141	0.01649	0.38111
9711	0.02921	0.02392	0.46670	**14150**	0.04839	0.01594	0.34259
9712	0.03063	0.02408	0.46221	**14624**	0.05353	0.01409	0.21136
9713	0.03655	0.02413	0.37756	**14639**	0.08375	0.01087	0.22219
9716	0.06358	0.01390	0.26072	**14778**	0.08035	0.01964	0.19889
9741	0.02109	0.02773	0.62146	**14786**	0.08719	0.01584	0.18194
9743	0.02320	0.02759	0.58357	**14920**	0.09946	0.01608	0.23021
9765	0.01164	0.03381	1.03818	**14955**	0.07500	0.02139	0.19285
9766	0.01207	0.03140	1.04907	**15287**	0.09250	0.01717	0.21564
9767	0.01440	0.03410	0.84133	**15301**	0.07661	0.02063	0.19400
9779	0.03163	0.02345	0.45701	**15761**	0.09085	0.01552	0.22853
9781	0.02268	0.02923	0.57983	**16117**	0.07787	0.01166	0.18566
9782	0.01806	0.03161	0.68298	**16258**	0.10540	0.01083	0.16429
9783	0.02002	0.03392	0.61318	**16706**	0.11607	0.01990	0.19821
9785	0.02128	0.03202	0.59391	**16726**	0.08957	0.01714	0.19632
9805	0.01179	0.03471	1.04866	**16729**	0.09152	0.01536	0.18230
9808	0.01721	0.03671	0.68215	**24095**	0.09970	0.01776	0.33745
9810	0.01874	0.03610	0.62904	**24242**	0.05112	0.01837	0.25037
9811	0.01094	0.03063	1.22893	**24386**	0.06662	0.02284	0.29846
9812	0.02044	0.03037	0.65780	**24510**	0.05095	0.02012	0.29607
9823	0.01899	0.03558	0.63795	**24612**	0.05235	0.02481	0.44853
9825	0.01236	0.03917	0.92568	**24619**	0.03241	0.02356	0.42190
9828	0.01477	0.04172	0.73890	**24665**	0.03523	0.02271	0.39535
9829	0.01280	0.03531	1.01393	**24703**	0.03827	0.02057	0.36379
10052	0.04478	0.01740	0.39557	**24741**	0.04210	0.03253	0.52754
10055	0.02234	0.02648	0.59584	**24787**	0.02447	0.02818	0.46779
10067	0.07197	0.01138	0.25202	**24788**	0.03002	0.02607	0.46261
10116	0.01256	0.02464	1.33036	**24789**	0.03126	0.02277	0.43252
10117	0.01228	0.02803	1.23881	**24806**	0.03446	0.03322	0.53440
10118	0.01908	0.03247	0.67438	**24830**	0.02409	0.02569	0.44969
10123	0.01134	0.03208	1.15720	**24862**	0.03099	0.02958	0.47364
10124	0.01237	0.03679	0.97107	**24863**	0.02729	0.02623	0.44387
11182	0.04323	0.01809	0.41337	**24864**	0.03029	0.03138	0.50238
11241	0.04601	0.01939	0.37988	**24865**	0.02550	0.03569	0.55298

Element	Damage (mm/mm² bone tissue)	BMU Activation Frequency (BMUs/mm²/day)	Density (g/cm³)	Element	Damage (mm/mm² bone tissue)	BMU Activation Frequency (BMUs/mm²/day)	Density (g/cm³)
11313	0.02276	0.03473	0.53915	**24866**	0.02202	0.03967	0.68016
11600	0.06111	0.02130	0.26612	**24867**	0.01678	0.04114	0.81048
11738	0.07886	0.01197	0.23055	**24874**	0.01377	0.01915	0.36442
11791	0.08493	0.00963	0.21803	**24875**	0.04102	0.02085	0.40012
11881	0.06407	0.01337	0.29880	**24906**	0.03692	0.03677	0.59139
Average	0.04452	0.02352	0.47253				
7M Postflight							
8026	0.06787	0.01564	0.27311	**12339**	0.04792	0.01871	0.39530
8320	0.03476	0.01808	0.45749	**12347**	0.04863	0.01843	0.39839
8321	0.03252	0.01971	0.48297	**12764**	0.07226	0.01923	0.23928
8323	0.03362	0.01928	0.46730	**13072**	0.08800	0.01685	0.20621
8324	0.03579	0.01642	0.44900	**13092**	0.07814	0.01954	0.23895
8325	0.01687	0.02948	0.76469	**13097**	0.06592	0.02033	0.26788
8326	0.02355	0.02605	0.58348	**13211**	0.09139	0.01507	0.20165
8327	0.02591	0.02261	0.55951	**13229**	0.09027	0.01447	0.21102
9331	0.05556	0.01575	0.28968	**13383**	0.07405	0.01725	0.24356
9562	0.05307	0.01591	0.38419	**13391**	0.05828	0.02032	0.29826
9606	0.06248	0.01222	0.28914	**13393**	0.06339	0.02101	0.27370
9608	0.04072	0.02014	0.37964	**13736**	0.08589	0.01729	0.21401
9709	0.03657	0.01832	0.44529	**14143**	0.05087	0.01881	0.38231
9711	0.03163	0.02188	0.46483	**14150**	0.05616	0.01941	0.34423
9712	0.03319	0.02016	0.45910	**14624**	0.08790	0.01851	0.21274
9713	0.03966	0.02077	0.37480	**14639**	0.08489	0.01483	0.22488
9716	0.06857	0.01137	0.26129	**14778**	0.09248	0.01539	0.19736
9741	0.02280	0.02499	0.61882	**14786**	0.10554	0.01472	0.18126
9743	0.02505	0.02338	0.58020	**14920**	0.07946	0.01621	0.23096
9765	0.01255	0.03020	1.03466	**14955**	0.09777	0.01602	0.19117
9766	0.01301	0.02809	1.04590	**15287**	0.08005	0.02069	0.21699
9767	0.01552	0.03020	0.83775	**15301**	0.09573	0.01721	0.19270
9779	0.03426	0.01858	0.45428	**15761**	0.08137	0.01968	0.23033
9781	0.02453	0.02440	0.57638	**16117**	0.11005	0.01606	0.18756
9782	0.01955	0.02750	0.67972	**16258**	0.11992	0.01826	0.16750
9783	0.02161	0.02843	0.60899	**16706**	0.09567	0.01404	0.19607
9785	0.02297	0.02684	0.59011	**16726**	0.09719	0.01488	0.19570
9805	0.01267	0.03038	1.04486	**16729**	0.10544	0.01519	0.18254
9808	0.01857	0.03116	0.67758	**24095**	0.05417	0.01784	0.33876
9810	0.02024	0.03025	0.62449	**24242**	0.07162	0.01309	0.24945
9811	0.01172	0.02751	1.22594	**24386**	0.05496	0.01608	0.29646
9812	0.02196	0.02599	0.65421	**24510**	0.05639	0.01508	0.29499
9823	0.02045	0.03030	0.63366	**24612**	0.03495	0.01933	0.44550
9825	0.01328	0.03452	0.92133	**24619**	0.03794	0.01870	0.41940
9828	0.01589	0.03651	0.73400	**24665**	0.04120	0.01764	0.39310
9829	0.01373	0.03059	1.00948	**24703**	0.04541	0.01644	0.36231
10052	0.04724	0.01937	0.39679	**24741**	0.02632	0.02660	0.52342
10055	0.02420	0.02297	0.59267	**24787**	0.03229	0.02217	0.46417
10067	0.07593	0.01718	0.25478	**24788**	0.03360	0.02151	0.45985
10116	0.01339	0.02165	1.32770	**24789**	0.03707	0.02048	0.43115
10117	0.01312	0.02462	1.23566	**24806**	0.02591	0.02697	0.53009
10118	0.02051	0.02800	0.67060	**24830**	0.03341	0.02310	0.44771
10123	0.01217	0.02841	1.15380	**24862**	0.02943	0.02708	0.47131
10124	0.01329	0.03244	0.96690	**24863**	0.03267	0.02502	0.44244
11182	0.04559	0.01905	0.41419	**24864**	0.02747	0.02729	0.49924
11241	0.04848	0.01972	0.38036	**24865**	0.02370	0.03006	0.54867
11313	0.02449	0.02909	0.53492	**24866**	0.01805	0.03409	0.67553
11600	0.06452	0.02030	0.26551	**24867**	0.01479	0.03617	0.80583
11738	0.08234	0.01873	0.23353	**24874**	0.04387	0.02165	0.36564
11791	0.08856	0.01775	0.22210	**24875**	0.03970	0.02132	0.40006
11881	0.05931	0.01732	0.30174	**24906**	0.02152	0.03204	0.58740
Average	0.04732	0.02175	0.47122				
8M Postflight							
8026	0.07086	0.01900	0.27461	**12339**	0.05054	0.01707	0.39471
8320	0.03685	0.02122	0.45983	**12347**	0.05130	0.01624	0.39754
8321	0.03450	0.02201	0.48490	**12764**	0.07660	0.01777	0.23852
8323	0.03570	0.02159	0.46920	**13072**	0.09341	0.01558	0.20549
8324	0.03808	0.01951	0.45170	**13092**	0.08295	0.01415	0.23671
8325	0.01798	0.03122	0.76554	**13097**	0.06959	0.01738	0.26642
8326	0.02504	0.02808	0.58472	**13211**	0.09757	0.01307	0.20090
8327	0.02762	0.02434	0.56097	**13229**	0.09651	0.01161	0.20968
9331	0.05934	0.01625	0.29113	**13383**	0.07852	0.01558	0.24252
9562	0.05556	0.01655	0.38489	**13391**	0.06176	0.01715	0.29688

Element	Damage (mm/mm² bone tissue)	BMU Activation Frequency (BMUs/mm²/day)	Density (g/cm³)	Element	Damage (mm/mm² bone tissue)	BMU Activation Frequency (BMUs/mm²/day)	Density (g/cm³)
9606	0.06560	0.01720	0.29250	**13393**	0.06692	0.01812	0.27221
9608	0.04349	0.01908	0.37979	**13736**	0.09144	0.01425	0.21254
9709	0.03898	0.01958	0.44673	**14143**	0.05368	0.01596	0.38105
9711	0.03362	0.02341	0.46618	**14150**	0.05932	0.01571	0.34246
9712	0.03530	0.02207	0.46074	**14624**	0.09345	0.01415	0.21090
9713	0.04208	0.02305	0.37654	**14639**	0.08997	0.01379	0.22415
9716	0.07238	0.01556	0.26423	**14778**	0.09844	0.01398	0.19713
9741	0.02436	0.02543	0.61917	**14786**	0.11228	0.01258	0.18050
9743	0.02675	0.02406	0.58110	**14920**	0.08439	0.01509	0.23005
9765	0.01339	0.03108	1.03471	**14955**	0.10351	0.01485	0.19089
9766	0.01388	0.02872	1.04595	**15287**	0.08569	0.01470	0.21468
9767	0.01653	0.03117	0.83804	**15301**	0.10203	0.01432	0.19125
9779	0.03642	0.02129	0.45648	**15761**	0.08647	0.01497	0.22791
9781	0.02607	0.02699	0.57807	**16117**	0.11685	0.01188	0.18557
9782	0.02086	0.02909	0.68063	**16258**	0.12735	0.01310	0.16513
9783	0.02297	0.03075	0.61016	**16706**	0.10115	0.01444	0.19652
9785	0.02441	0.02905	0.59139	**16726**	0.10281	0.01461	0.19543
9805	0.01346	0.03235	1.04553	**16729**	0.11168	0.01424	0.18178
9808	0.01973	0.03339	0.67840	**24095**	0.05695	0.01857	0.33915
9810	0.02151	0.03280	0.62565	**24242**	0.07575	0.01620	0.25110
9811	0.01244	0.02872	1.22617	**24386**	0.05830	0.01873	0.29832
9812	0.02332	0.02725	0.65507	**24510**	0.05972	0.01889	0.29721
9823	0.02173	0.03194	0.63444	**24612**	0.03722	0.02077	0.44706
9825	0.01410	0.03641	0.92160	**24619**	0.04039	0.01978	0.42072
9828	0.01687	0.03815	0.73402	**24665**	0.04382	0.01934	0.39466
9829	0.01457	0.03226	1.00976	**24703**	0.04812	0.01955	0.36442
10052	0.04972	0.01781	0.39632	**24741**	0.02796	0.02818	0.52438
10055	0.02587	0.02364	0.59328	**24787**	0.03427	0.02419	0.46557
10067	0.07966	0.01592	0.25443	**24788**	0.03552	0.02429	0.46163
10116	0.01415	0.02304	1.32827	**24789**	0.03900	0.02404	0.43322
10117	0.01390	0.02599	1.23602	**24806**	0.02750	0.02902	0.53124
10118	0.02178	0.02932	0.67130	**24830**	0.03517	0.02683	0.44954
10123	0.01292	0.03003	1.15425	**24862**	0.03094	0.03121	0.47294
10124	0.01412	0.03390	0.96701	**24863**	0.03429	0.02932	0.44423
11182	0.04804	0.01751	0.41365	**24864**	0.02899	0.03061	0.50070
11241	0.05112	0.01801	0.37966	**24865**	0.02510	0.03273	0.54975
11313	0.02604	0.03032	0.53554	**24866**	0.01911	0.03689	0.67639
11600	0.06856	0.01734	0.26450	**24867**	0.01567	0.03834	0.80613
11738	0.08760	0.01282	0.23103	**24874**	0.04613	0.02274	0.36644
11791	0.09404	0.01227	0.21981	**24875**	0.04164	0.02472	0.40173
11881	0.06233	0.01844	0.30215	**24906**	0.02272	0.03549	0.58860
Average	0.05016	0.02219	0.47159				
9M Postflight							
8026	0.07575	0.01286	0.27101	**12339**	0.05320	0.01647	0.39440
8320	0.03920	0.01834	0.45784	**12347**	0.05402	0.01571	0.39731
8321	0.03659	0.02023	0.48343	**12764**	0.08068	0.01778	0.23833
8323	0.03790	0.01968	0.46768	**13072**	0.09821	0.01588	0.20567
8324	0.04046	0.01799	0.45045	**13092**	0.08786	0.01420	0.23660
8325	0.01908	0.02952	0.76358	**13097**	0.07413	0.01484	0.26502
8326	0.02657	0.02601	0.58274	**13211**	0.10273	0.01431	0.20145
8327	0.02934	0.02304	0.55969	**13229**	0.10223	0.01188	0.20993
9331	0.06309	0.01682	0.29078	**13383**	0.08374	0.01283	0.24127
9562	0.05866	0.01352	0.38334	**13391**	0.06555	0.01634	0.29609
9606	0.07011	0.01249	0.28951	**13393**	0.07135	0.01498	0.27075
9608	0.04629	0.01879	0.37934	**13736**	0.09652	0.01441	0.21269
9709	0.04143	0.01871	0.44598	**14143**	0.05652	0.01560	0.38097
9711	0.03580	0.02096	0.46461	**14150**	0.06249	0.01544	0.34248
9712	0.03751	0.02036	0.45950	**14624**	0.09863	0.01433	0.21104
9713	0.04477	0.02065	0.37486	**14639**	0.09581	0.01131	0.22301
9716	0.07731	0.01251	0.26187	**14778**	0.10337	0.01557	0.19763
9741	0.02593	0.02408	0.61797	**14786**	0.11819	0.01325	0.18093
9743	0.02840	0.02341	0.58028	**14920**	0.08934	0.01398	0.22952
9765	0.01420	0.02978	1.03305	**14955**	0.10842	0.01619	0.19135
9766	0.01473	0.02760	1.04461	**15287**	0.09024	0.01706	0.21555
9767	0.01752	0.02979	0.83635	**15301**	0.10682	0.01614	0.19223
9779	0.03867	0.01974	0.45502	**15761**	0.09113	0.01501	0.22814
9781	0.02764	0.02500	0.57616	**16117**	0.12315	0.01178	0.18578
9782	0.02216	0.02749	0.67883	**16258**	0.13438	0.01256	0.16494
9783	0.02432	0.02908	0.60806	**16706**	0.10642	0.01478	0.19650
9785	0.02586	0.02740	0.58947	**16726**	0.10843	0.01369	0.19506

Element	Damage (mm/mm² bone tissue)	BMU Activation Frequency (BMUs/mm²/day)	Density (g/cm³)	Element	Damage (mm/mm² bone tissue)	BMU Activation Frequency (BMUs/mm²/day)	Density (g/cm³)
9805	0.01421	0.03077	1.04333	**16729**	0.11792	0.01303	0.18133
9808	0.02088	0.03171	0.67607	**24095**	0.06019	0.01597	0.33760
9810	0.02277	0.03104	0.62328	**24242**	0.08035	0.01393	0.24975
9811	0.01314	0.02748	1.22444	**24386**	0.06181	0.01771	0.29711
9812	0.02466	0.02602	0.65371	**24510**	0.06344	0.01641	0.29521
9823	0.02298	0.03071	0.63245	**24612**	0.03944	0.02052	0.44627
9825	0.01489	0.03480	0.91896	**24619**	0.04280	0.01950	0.42003
9828	0.01782	0.03665	0.73129	**24665**	0.04644	0.01878	0.39371
9829	0.01537	0.03104	1.00764	**24703**	0.05110	0.01740	0.36268
10052	0.05242	0.01645	0.39558	**24741**	0.02955	0.02748	0.52286
10055	0.02754	0.02241	0.59244	**24787**	0.03621	0.02344	0.46427
10067	0.08464	0.01281	0.25294	**24788**	0.03755	0.02221	0.45974
10116	0.01488	0.02216	1.32690	**24789**	0.04131	0.02022	0.43066
10117	0.01464	0.02504	1.23443	**24806**	0.02903	0.02805	0.52950
10118	0.02303	0.02797	0.66971	**24830**	0.03728	0.02261	0.44671
10123	0.01363	0.02879	1.15228	**24862**	0.03279	0.02618	0.46947
10124	0.01491	0.03267	0.96475	**24863**	0.03641	0.02362	0.44072
11182	0.05060	0.01647	0.41315	**24864**	0.03068	0.02724	0.49788
11241	0.05381	0.01725	0.37928	**24865**	0.02652	0.03066	0.54722
11313	0.02754	0.02964	0.53387	**24866**	0.02016	0.03464	0.67340
11600	0.07215	0.01849	0.26479	**24867**	0.01653	0.03643	0.80316
11738	0.09264	0.01321	0.23145	**24874**	0.04907	0.01896	0.36398
11791	0.09980	0.01168	0.21972	**24875**	0.04425	0.01956	0.39869
11881	0.06647	0.01419	0.29968	**24906**	0.02400	0.03212	0.58533
Average	0.05307	0.02077	0.47029				
10M Postflight							
8026	0.07961	0.01456	0.27226	**12339**	0.05584	0.01576	0.39417
8320	0.04160	0.01758	0.45722	**12347**	0.05666	0.01536	0.39720
8321	0.03879	0.01891	0.48233	**12764**	0.08504	0.01601	0.23759
8323	0.04020	0.01847	0.46668	**13072**	0.10358	0.01403	0.20496
8324	0.04302	0.01638	0.44921	**13092**	0.09211	0.01467	0.23685
8325	0.02022	0.02805	0.76171	**13097**	0.07775	0.01654	0.26588
8326	0.02816	0.02471	0.58127	**13211**	0.10874	0.01222	0.20054
8327	0.03115	0.02156	0.55824	**13229**	0.10797	0.01161	0.20971
9331	0.06727	0.01439	0.28925	**13383**	0.08808	0.01459	0.24204
9562	0.06148	0.01443	0.38380	**13391**	0.06897	0.01645	0.29610
9606	0.07435	0.01268	0.28964	**13393**	0.07480	0.01733	0.27178
9608	0.04912	0.01780	0.37842	**13736**	0.10171	0.01384	0.21234
9709	0.04401	0.01751	0.44469	**14143**	0.05924	0.01541	0.38092
9711	0.03798	0.02056	0.46386	**14150**	0.06544	0.01557	0.34253
9712	0.03981	0.01936	0.45838	**14624**	0.10356	0.01444	0.21084
9713	0.04752	0.01993	0.37381	**14639**	0.10082	0.01268	0.22366
9716	0.08224	0.01146	0.26149	**14778**	0.10946	0.01261	0.19638
9741	0.02752	0.02314	0.61675	**14786**	0.12477	0.01211	0.18023
9743	0.03013	0.02193	0.57877	**14920**	0.09418	0.01371	0.22945
9765	0.01503	0.02859	1.03130	**14955**	0.11441	0.01323	0.19017
9766	0.01558	0.02654	1.04308	**15287**	0.09511	0.01500	0.21470
9767	0.01853	0.02845	0.83454	**15301**	0.11261	0.01365	0.19120
9779	0.04107	0.01807	0.45375	**15761**	0.09548	0.01526	0.22818
9781	0.02931	0.02351	0.57462	**16117**	0.12888	0.01244	0.18597
9782	0.02351	0.02602	0.67714	**16258**	0.14022	0.01352	0.16538
9783	0.02576	0.02719	0.60599	**16706**	0.11257	0.01252	0.19537
9785	0.02740	0.02562	0.58761	**16726**	0.11428	0.01295	0.19469
9805	0.01500	0.02930	1.04127	**16729**	0.12407	0.01288	0.18124
9808	0.02209	0.02982	0.67373	**24095**	0.06331	0.01574	0.33774
9810	0.02411	0.02906	0.62095	**24242**	0.08529	0.01246	0.24932
9811	0.01385	0.02640	1.22281	**24386**	0.06575	0.01510	0.29589
9812	0.02607	0.02447	0.65212	**24510**	0.06744	0.01448	0.29446
9823	0.02431	0.02868	0.63016	**24612**	0.04185	0.01825	0.44467
9825	0.01571	0.03309	0.9164	**24619**	0.04540	0.01743	0.41863
9828	0.01882	0.03467	0.72843	**24665**	0.04929	0.01659	0.39236
9829	0.01620	0.02952	1.00532	**24703**	0.05423	0.01597	0.36181
10052	0.05499	0.01630	0.39565	**24741**	0.03128	0.02503	0.52070
10055	0.02924	0.02150	0.59134	**24787**	0.03835	0.02102	0.46248
10067	0.08861	0.01496	0.25371	**24788**	0.03970	0.02066	0.45845
10116	0.01563	0.02121	1.32549	**24789**	0.04362	0.01994	0.43012
10117	0.01540	0.02394	1.23276	**24806**	0.03072	0.02550	0.52731
10118	0.02433	0.02637	0.66795	**24830**	0.03939	0.02246	0.44606
10123	0.01437	0.02752	1.15036	**24862**	0.03462	0.02633	0.46867
10124	0.01573	0.03108	0.96237	**24863**	0.03842	0.02452	0.44044

Element	Damage (mm/mm^2 bone tissue)	BMU Activation Frequency ($BMUs/mm^2/day$)	Density (g/cm^3)	Element	Damage (mm/mm^2 bone tissue)	BMU Activation Frequency ($BMUs/mm^2/day$)	Density (g/cm^3)
11182	0.05310	0.01606	0.41313	**24864**	0.03242	0.02619	0.49648
11241	0.05648	0.01654	0.37909	**24865**	0.02804	0.02864	0.54503
11313	0.02916	0.02723	0.53153	**24866**	0.02129	0.03267	0.67086
11600	0.07607	0.01637	0.26375	**24867**	0.01743	0.03458	0.80044
11738	0.09707	0.01401	0.23170	**24874**	0.05172	0.01972	0.36405
11791	0.10445	0.01339	0.22042	**24875**	0.04665	0.02067	0.39879
11881	0.06995	0.01561	0.30050	**24906**	0.02535	0.03083	0.58337
Average	0.05597	0.01986	0.46936				
11M Postflight							
8026	0.08348	0.01415	0.27206	**12339**	0.05854	0.01499	0.39380
8320	0.04385	0.01781	0.45720	**12347**	0.05941	0.01432	0.39670
8321	0.04086	0.01902	0.48218	**12764**	0.08937	0.01578	0.23727
8323	0.04237	0.01857	0.46655	**13072**	0.10883	0.01398	0.20473
8324	0.04540	0.01676	0.44937	**13092**	0.09711	0.01270	0.23581
8325	0.02131	0.02792	0.76073	**13097**	0.08192	0.01451	0.26469
8326	0.02967	0.02463	0.58058	**13211**	0.11456	0.01209	0.20044
8327	0.03287	0.02148	0.55778	**13229**	0.11408	0.01050	0.20907
9331	0.07117	0.01453	0.28938	**13383**	0.09297	0.01278	0.24093
9562	0.06435	0.01342	0.38335	**13391**	0.07266	0.01511	0.29525
9606	0.07822	0.01307	0.28995	**13393**	0.07888	0.01476	0.27036
9608	0.05195	0.01693	0.37781	**13736**	0.10718	0.01271	0.21167
9709	0.04650	0.01725	0.44423	**14143**	0.06212	0.01415	0.38029
9711	0.04010	0.01998	0.46324	**14150**	0.06867	0.01398	0.34167
9712	0.04200	0.01914	0.45796	**14624**	0.10917	0.01254	0.20985
9713	0.05014	0.01965	0.37327	**14639**	0.10631	0.01132	0.22282
9716	0.08662	0.01239	0.26210	**14778**	0.11507	0.01299	0.19656
9741	0.02907	0.02265	0.61586	**14786**	0.13143	0.01129	0.17982
9743	0.03181	0.02159	0.57814	**14920**	0.09914	0.01317	0.22890
9765	0.01582	0.02833	1.03011	**14955**	0.11996	0.01360	0.19030
9766	0.01641	0.02627	1.04201	**15287**	0.10038	0.01393	0.21418
9767	0.01951	0.02816	0.83341	**15301**	0.11839	0.01346	0.19094
9779	0.04331	0.01843	0.45376	**15761**	0.10052	0.01339	0.22706
9781	0.03087	0.02362	0.57412	**16117**	0.13572	0.01055	0.18492
9782	0.02480	0.02589	0.67633	**16258**	0.14772	0.01135	0.16425
9783	0.02711	0.02728	0.60518	**16706**	0.11818	0.01269	0.19551
9785	0.02884	0.02569	0.58693	**16726**	0.12005	0.01258	0.19434
9805	0.01574	0.02933	1.04018	**16729**	0.13044	0.01217	0.18069
9808	0.02323	0.02983	0.67263	**24095**	0.06634	0.01553	0.33753
9810	0.02536	0.02915	0.61998	**24242**	0.08964	0.01367	0.24973
9811	0.01452	0.02632	1.22181	**24386**	0.06922	0.01627	0.29639
9812	0.02742	0.02427	0.65143	**24510**	0.07094	0.01592	0.29503
9823	0.02557	0.02854	0.62918	**24612**	0.04414	0.01851	0.44464
9825	0.01648	0.03300	0.91496	**24619**	0.04788	0.01760	0.41857
9828	0.01977	0.03447	0.72677	**24665**	0.05195	0.01706	0.39249
9829	0.01700	0.02945	1.00399	**24703**	0.05711	0.01653	0.36199
10052	0.05764	0.01534	0.39517	**24741**	0.03291	0.02521	0.52014
10055	0.03090	0.02104	0.59063	**24787**	0.04034	0.02149	0.46232
10067	0.09316	0.01266	0.25258	**24788**	0.04170	0.02095	0.45826
10116	0.01635	0.02127	1.32478	**24789**	0.04577	0.01989	0.42981
10117	0.01613	0.02394	1.23184	**24806**	0.03230	0.02582	0.52681
10118	0.02558	0.02616	0.66712	**24830**	0.04135	0.02230	0.44549
10123	0.01507	0.02749	1.14931	**24862**	0.03632	0.02596	0.46772
10124	0.01651	0.03095	0.96098	**24863**	0.04031	0.02385	0.43948
11182	0.05565	0.01523	0.41271	**24864**	0.03404	0.02618	0.49574
11241	0.05920	0.01577	0.37865	**24865**	0.02945	0.02880	0.54417
11313	0.03069	0.02720	0.53068	**24866**	0.02234	0.03272	0.66963
11600	0.08003	0.01580	0.26340	**24867**	0.01828	0.03447	0.79891
11738	0.10244	0.01160	0.23046	**24874**	0.05437	0.01868	0.36328
11791	0.11030	0.01075	0.21908	**24875**	0.04896	0.01987	0.39804
11881	0.07353	0.01473	0.29987	**24906**	0.02659	0.03078	0.58225
Average	0.05890	0.01945	0.46876				
12M Postflight							
8026	0.08787	0.01268	0.27094	**12339**	0.06125	0.01442	0.39352
8320	0.04618	0.01663	0.45619	**12347**	0.06214	0.01392	0.39651
8321	0.04296	0.01808	0.48124	**12764**	0.09377	0.01484	0.23671
8323	0.04458	0.01762	0.46562	**13072**	0.11420	0.01299	0.20427
8324	0.04782	0.01597	0.44857	**13092**	0.10182	0.01288	0.23575
8325	0.02238	0.02689	0.75909	**13097**	0.08611	0.01404	0.26424
8326	0.03119	0.02352	0.57916	**13211**	0.12032	0.01171	0.20020
8327	0.03459	0.02067	0.55674	**13229**	0.11995	0.01050	0.20901

Element	Damage (mm/mm^2 bone tissue)	BMU Activation Frequency ($BMUs/mm^2/day$)	Density (g/cm^3)	Element	Damage (mm/mm^2 bone tissue)	BMU Activation Frequency ($BMUs/mm^2/day$)	Density (g/cm^3)
9331	0.07505	0.01431	0.28892	**13383**	0.09788	0.01223	0.24056
9562	0.06734	0.01269	0.38292	**13391**	0.07631	0.01485	0.29479
9606	0.08251	0.01177	0.28898	**13393**	0.08293	0.01442	0.27002
9608	0.05475	0.01660	0.37737	**13736**	0.11251	0.01245	0.21150
9709	0.04900	0.01662	0.44348	**14143**	0.06497	0.01384	0.38017
9711	0.04226	0.01905	0.46229	**14150**	0.07183	0.01377	0.34161
9712	0.04422	0.01832	0.45706	**14624**	0.11437	0.01277	0.20987
9713	0.05284	0.01862	0.37219	**14639**	0.11189	0.01076	0.22244
9716	0.09144	0.01127	0.26116	**14778**	0.12075	0.01240	0.19619
9741	0.03061	0.02182	0.61473	**14786**	0.13785	0.01115	0.17976
9743	0.03347	0.02095	0.57721	**14920**	0.10423	0.01228	0.22836
9765	0.01660	0.02746	1.02849	**14955**	0.12565	0.01279	0.18990
9766	0.01722	0.02546	1.04060	**15287**	0.10522	0.01427	0.21412
9767	0.02047	0.02722	0.83181	**15301**	0.12400	0.01294	0.19068
9779	0.04558	0.01750	0.45282	**15761**	0.10526	0.01324	0.22700
9781	0.03245	0.02251	0.57277	**16117**	0.14202	0.01058	0.18500
9782	0.02608	0.02492	0.67488	**16258**	0.15450	0.01153	0.16422
9783	0.02847	0.02617	0.60350	**16706**	0.12397	0.01211	0.19514
9785	0.03030	0.02460	0.58543	**16726**	0.12604	0.01168	0.19390
9805	0.01647	0.02835	1.03839	**16729**	0.13696	0.01137	0.18027
9808	0.02437	0.02869	0.67073	**24095**	0.06959	0.01418	0.33677
9810	0.02662	0.02797	0.61811	**24242**	0.09452	0.01185	0.24870
9811	0.01519	0.02555	1.22031	**24386**	0.07293	0.01493	0.29536
9812	0.02876	0.02339	0.65023	**24510**	0.07479	0.01422	0.29376
9823	0.02683	0.02755	0.62752	**24612**	0.04641	0.01786	0.44385
9825	0.01724	0.03192	0.91280	**24619**	0.05036	0.01693	0.41787
9828	0.02071	0.03333	0.72444	**24665**	0.05464	0.01627	0.39169
9829	0.01777	0.02855	1.00210	**24703**	0.06013	0.01540	0.36101
10052	0.06034	0.01469	0.39480	**24741**	0.03454	0.02426	0.51874
10055	0.03256	0.02031	0.58970	**24787**	0.04234	0.02052	0.46115
10067	0.09770	0.01248	0.25237	**24788**	0.04376	0.01979	0.45705
10116	0.01706	0.02072	1.32361	**24789**	0.04806	0.01850	0.42858
10117	0.01685	0.02328	1.23046	**24806**	0.03387	0.02476	0.52531
10118	0.02683	0.02521	0.66573	**24830**	0.04344	0.02074	0.44404
10123	0.01575	0.02669	1.14769	**24862**	0.03814	0.02416	0.46590
10124	0.01727	0.03002	0.95902	**24863**	0.04236	0.02208	0.43786
11182	0.05824	0.01454	0.41239	**24864**	0.03573	0.02464	0.49402
11241	0.06196	0.01504	0.37828	**24865**	0.03089	0.02746	0.54229
11313	0.03221	0.02627	0.52914	**24866**	0.02340	0.03135	0.66741
11600	0.08389	0.01547	0.26307	**24867**	0.01912	0.03325	0.79658
11738	0.10733	0.01205	0.23067	**24874**	0.05716	0.01765	0.36230
11791	0.11567	0.01114	0.21925	**24875**	0.05146	0.01844	0.39681
11881	0.07737	0.01360	0.29899	**24906**	0.02787	0.02918	0.58012
Average	0.06184	0.01865	0.46781				